

**CRC Report No. CM-138-16-2**

**COMPARISON OF AMBIENT  
TEMPERATURES FROM 'DONER  
REPORT' TO MODERN DAY AMBIENT  
TEMPERATURES FOR THE SAME  
GEOGRAPHIC AREAS**

**December 2018**



**COORDINATING RESEARCH COUNCIL, INC.  
5755 NORTH POINT PARKWAY • SUITE 265 • ALPHARETTA, GA 30022**

**The Coordinating Research Council, Inc. (CRC) is a non-profit corporation supported by the petroleum and automotive equipment industries. CRC operates through committees made up of technical experts from industry and government who voluntarily participate. The four main areas of research within CRC are: air pollution (atmospheric and engineering studies); aviation fuels, lubricants, and equipment performance; heavy-duty vehicle fuels, lubricants, and equipment performance (e.g., diesel trucks); and light-duty vehicle fuels, lubricants, and equipment performance (e.g., passenger cars). CRC's function is to provide the mechanism for joint research conducted by the two industries that will help in determining the optimum combination of petroleum products and automotive equipment. CRC's work is limited to research that is mutually beneficial to the two industries involved. The final results of the research conducted by, or under the auspices of, CRC are available to the public.**

**This report was prepared by Desert Research Institute (DRI) as an account of work sponsored by the Coordinating Research Council (CRC). Neither CRC, members of CRC, DRI nor any person acting on their behalf: (1) makes any warranty express or implied, with respect to the use of any information, apparatus, method, or process disclosed in this report, or (2) assumes any liabilities with respect to use of, inability to use, or damages resulting from the use or inability to use, any information, apparatus, method, or process disclosed in this report.**

FINAL REPORT

CRC Project CM-138-16-2

**Comparison of Ambient Temperatures from ‘Doner Report’  
to Modern Day Ambient Temperatures for the Same  
Geographic Areas**

Prepared by:

S. Kent Hoekman  
Daniel McEvoy  
David Simeral  
Paul Fremeau

Desert Research Institute  
Reno, NV 89512



November 19, 2018

# Contents

1	Executive Summary .....	1
2	Introduction and Background .....	5
2.1	Doner Methodology .....	6
2.2	Project Objectives .....	7
3	Methodology .....	7
3.1	Selection of weather stations.....	7
3.2	Acquisition of temperature data .....	8
3.3	Data processing and acceptance criteria.....	9
3.4	Data analysis and display methods.....	13
4	Results and Discussion .....	14
4.1	90 <sup>th</sup> Percentile 1-hr max. temperature .....	15
4.1.1	Dot maps and interpolated maps.....	15
4.1.2	Histograms .....	15
4.1.3	Statistical analysis of temperature differences.....	18
4.2	10 <sup>th</sup> Percentile 1-hr min. temperature.....	20
4.2.1	Dot maps and interpolated maps.....	20
4.2.2	Histograms .....	20
4.2.3	Statistical analysis of temperature differences.....	22
4.3	10 <sup>th</sup> Percentile 6-hr min. temperature.....	24
4.3.1	Dot maps and interpolated maps.....	24
4.3.2	Histograms .....	26
4.3.3	Statistical analysis of temperature differences.....	27
5	Conclusions.....	28
6	Recommendations.....	30
7	References.....	32

## List of Figures

Figure 1. Hourly temperature data from Eau Claire, WI (WBAN ID 14991) for 1950 generated using the MRCC’s cli-MATE tool ( <a href="http://mrcc.isws.illinois.edu/CLIMATE/">http://mrcc.isws.illinois.edu/CLIMATE/</a> ). .....	9
Figure 2. Data completeness of January 1-hr max. temperature values from 317 weather stations recording data during the 20-year Doner era (top panel) and the 20-year Modern era (bottom panel). .....	10
Figure 3. Locations of the 228 weather stations used in this study. Numbers in circles indicate the number of stations in each PADD.....	12
Figure 4. Dot maps showing differences in 90 <sup>th</sup> percentile 1-hr max. temperature between Doner and Modern eras during March (left) and October (right). .....	16
Figure 5. Interpolated maps showing differences in 90 <sup>th</sup> percentile 1-hr max. temperature between Doner and Modern eras during March (left) and October (right). .....	16
Figure 6. Numbers of weather stations throughout the U.S. showing differences in 90 <sup>th</sup> percentile 1-hr max. temperature between the Doner and Modern eras (by month). .....	17
Figure 7. Magnitude and significance of 90 <sup>th</sup> percentile 1-hr max. temperature differences between the Doner era (1950-1969) and the Modern era (1996-2015) - by month and PADD.....	19
Figure 8. Dot maps showing differences in 10 <sup>th</sup> percentile 1-hr min. temperature between Doner and Modern eras during March (left) and October (right). .....	21
Figure 9. Interpolated maps showing differences in 10 <sup>th</sup> percentile 1-hr min. temperature between Doner and Modern eras during March (left) and October (right). .....	21
Figure 10. Numbers of weather stations throughout the U.S. showing differences in 10 <sup>th</sup> percentile 1-hr min. temperature between the Doner and Modern eras (by month). .....	22
Figure 11. Magnitude and significance of 10 <sup>th</sup> percentile 1-hr min. temperature differences between the Doner era (1950-1969) and the Modern era (1996-2015) - by month and PADD.....	23
Figure 12. Dot maps showing differences in 10 <sup>th</sup> percentile 6-hr min. temperature between Doner and Modern eras during March (left) and October (right). .....	25
Figure 13. Interpolated maps showing differences in 10 <sup>th</sup> percentile 6-hr min. temperature between Doner and Modern eras during March (left) and October (right). .....	25
Figure 14. Numbers of weather stations throughout the U.S. showing differences in 10 <sup>th</sup> percentile 6-hr min. temperature between the Doner and Modern eras (by month). .....	26
Figure 15. Magnitude and significance of 10 <sup>th</sup> percentile 6-hr min. temperature differences between the Doner era (1950-1969) and the Modern eras (1996-2015) – by month and PADD. ....	28
Figure 16. Elevational distribution of observing stations from the western U.S. The overall mean station elevation was ~2400 ft. ....	30
Figure 17. PRISM 30-year normal annual maximum temperature downloaded from <a href="http://prism.oregonstate.edu/normals/">http://prism.oregonstate.edu/normals/</a> .....	32

## List of Tables

Table 1. Vapor Pressure Class Requirements in ASTM D4814 .....	5
Table 2. Vapor Lock Protection Class Requirements in ASTM D4814 .....	5
Table 3. ASTM D4814 Guidance for Selecting Alpha-Numeric Designations for Gasoline Volatility	6
Table 4. Average Percent Data Completeness of Temperature Records from 317 Weather Stations .	11
Table 5. Number of Stations (Satisfying 50% Data Completeness Threshold) used to Compare Temperature Data between the Doner and Modern Eras .....	12
Table 6. Differences and associated p-values in 90 <sup>th</sup> percentile 1-hr max. temperature between Doner and Modern eras (Modern – Doner) .....	18
Table 7. Differences and associated p-values in 10 <sup>th</sup> percentile 1-hr min. temperature between Doner and Modern eras (Modern – Doner) .....	23
Table 8. Differences and associated p-values in 10 <sup>th</sup> percentile 6-hr min. temperature between Doner and Modern eras (Modern – Doner) .....	27

## Appendices

### Appendix I. Identification of Weather Stations used in the Doner Study and the Current Study

Appendix I-A. List of 340 Weather Stations Used in the Doner Study

Appendix I-B. List of 228 Weather Stations Used in the Current Study

### Appendix II. Monthly Temperature Metrics from Stations Satisfying the 50% Data Completeness Threshold during the Doner and Modern Eras

### Appendix III. Dot Maps Showing Temperature Differences between the Doner and Modern Eras for Each Weather Station

Appendix III-A. 90<sup>th</sup> Percentile 1-Hr Max. Temperature

Appendix III-B. 10<sup>th</sup> Percentile 1-Hr Min. Temperature

Appendix III-C. 10<sup>th</sup> Percentile 6-Hr Min. Temperature

### Appendix IV. Interpolated Temperature Maps Showing Differences between the Doner and Modern Eras

Appendix IV-A. 90<sup>th</sup> Percentile 1-Hr Max. Temperature

Appendix IV-B. 10<sup>th</sup> Percentile 1-Hr Min. Temperature

Appendix IV-C. 10<sup>th</sup> Percentile 6-Hr Min. Temperature

### Appendix V. Histograms Displaying Numbers of Weather Stations (by PADD) Showing Temperature Differences between the Doner and Modern Eras

Appendix V-A. 90<sup>th</sup> Percentile 1-Hr Max. Temperature

Appendix V-B. 10<sup>th</sup> Percentile 1-Hr Min. Temperature

Appendix V-C. 10<sup>th</sup> Percentile 6-Hr Min. Temperature

### Appendix VI. Average Monthly Values of Temperature Metrics in Doner Era, Modern Era, and Difference – By State

## List of Acronyms and Abbreviations

ACIS	Applied Climate Information System
CD	Climate Division (NOAA designation)
CONUS	Contiguous U.S. (48-states)
COOP	Cooperative Observer Program (network of weather stations)
CRC	Coordinating Research Council
DRI	Desert Research Institute
FAA	Federal Aviation Administration
Hr	Hour
ICAO	International Civil Aviation Organization
IDW	Inverse Distance Weighting
Max.	Maximum
Min.	Minimum
MRCC	Midwest Regional Climate Center
NCDC	National Climatic Data Center
NCEI	National Center for Environmental Information
NOAA	National Oceanic and Atmospheric Administration
PADD	Petroleum Administration for Defense District
PRISM	Parameter Regression on Independent Slopes Model
UHI	Urban Heat Island
VOC	Volatile Organic Compound
WBAN	Weather Bureau Army Navy
WMO	World Meteorological Organization

# 1 Executive Summary

U.S. gasoline volatility specifications and diesel fuel low temperature operability requirements defined by ASTM International (ASTM) vary geographically and temporally to account for differing temperature conditions. The underlying meteorological data upon which these specifications are based were compiled, analyzed, and documented in a 1972 report by John P. Doner – hence the name, “Doner Report.” The time period of record Doner used varied across the range of stations, but most fell within a 20-year window of 1950-1969, which is referred to here as the Doner Era.

Using cumulative frequency distribution plots of monthly-lumped temperature data, Doner derived several metrics to define the long-term average temperature conditions at each station. ASTM adopted three of these metrics in defining fuel specifications: (1) 90<sup>th</sup> percentile 1-hr maximum (max.) temperature, (2) 10<sup>th</sup> percentile 1-hr minimum (min.) temperature, and (3) 10<sup>th</sup> percentile 6-hr min. temperature. Gasoline volatility specifications are based on the 90<sup>th</sup> percentile 1-hr max. and the 10<sup>th</sup> percentile 6-hr min. temperatures, while low temperature operability requirements for diesel fuel are based on the 10<sup>th</sup> percentile 1-hr min. temperature. In the original Doner Report, ambient temperatures were not adjusted for altitude. The same approach was followed in this report.

Because many years have passed since the Doner Report was issued, it is of interest to update that report with more recent meteorological data to ensure that fuel volatility issues are being properly addressed. In this study, the original Doner procedures were followed as closely as possible with respect to selection of weather stations and data processing methods, while using a more recent 20-year window of temperature data (1996-2015), which is referred to here as the Modern Era. The objective was to determine when (month), where, and to what extent 10<sup>th</sup> percentile min. and 90<sup>th</sup> percentile max. temperatures have changed between the Doner era and the Modern era. These assessments were conducted for each of the three temperature metrics mentioned above that are used in defining ASTM fuel specifications.

The study did not delve into meteorological instrument improvements or any other sources of variation in the observed temperature extremes of the Doner and the Modern eras. It only identifies, reports, and analyzes a data set that is most comparable to the original data used by John Doner in his report. This study focused on extreme temperature metrics (90<sup>th</sup> percentile 1-hr max., 10<sup>th</sup> percentile 1-hr min., and 10<sup>th</sup> percentile 6-hr min.), which are relevant to ASTM fuel specifications. Those interested in broader climate change should consult the literature identified in the references.

Most of the 340 weather stations used in the Doner Report are located at airports and Air Force bases in areas that have experienced substantial urban development since the Doner Era. This introduces the possibility that the urban heat island (UHI) effect (an exaggerated warming in urban centers relative to surrounding rural areas) may have played some role in the observed temperature differences.

Archived digitized temperature data from both the Doner and Modern eras were compiled for all of the 340 Doner stations that are still available, in addition to 21 Hawaii stations not included in the original Doner study. Data acceptance criteria were then applied to identify those stations having sufficient data during both time periods to ensure a robust comparative analysis. A data completion threshold of 50% was applied, meaning that an individual station would be included in the analysis

only if it had at least 10-years of valid temperature data during both time periods. A total of 228 stations satisfied this 50% data completion requirement for at least one of the three temperature metrics considered.

The 1-hr max., 1-hr min., and 6-hr min. temperature values were obtained for each day at each station, and these data were then binned by month. Applying the same cumulative frequency distribution method as used by Doner, the 90<sup>th</sup> percentile 1-hr max., 10<sup>th</sup> percentile 1-hr min., and 10<sup>th</sup> percentile 6-hr min. temperature values were determined for each month, during both the Doner era (1950-1969) and the Modern era (1996-2015).

These processed temperature data were further analyzed and displayed in various ways to facilitate comparison of results between the Doner and Modern eras. Colored dot maps were prepared to illustrate each of the three temperature metrics for each month at each station, during both time periods. An inverse distance weighting (IDW) method was used to translate the dot maps into interpolated temperature maps. The dot maps and interpolated maps were further analyzed by quantifying the differences between the Doner and Modern eras. Such “difference maps” more clearly illustrate the locations and months where warming or cooling has occurred since the Doner era. These difference maps show that warming has occurred in the majority of locations and months, as determined by all three temperature metrics. These temperature differences, however, have considerable variability with respect to their magnitude, spatial extent, and month of occurrence. A smaller number of locations show cooling trends – particularly as defined by the 90<sup>th</sup> percentile 1-hr max. temperatures.

The variability in temperature changes between the Doner and Modern eras was further examined by developing histograms to depict the number of stations showing warming versus cooling as determined using each of the three temperature metrics. These data were also analyzed on a regional basis by grouping the weather stations by Petroleum Administration for Defense District (PADD) regions. In general, more stations showed warming than cooling trends, although this was not the case for every region and month.

Finally, the temperature differences for the 10<sup>th</sup> percentile min. and 90<sup>th</sup> percentile max. metrics observed between the Doner and Modern eras were analyzed statistically – both for the entire U.S. and for individual PADD regions (with Alaska and Hawaii being treated separately). A two-sided paired t-test was utilized to test the null hypothesis that there was no temperature difference between the two time periods. T-tests were conducted for each of the three temperature metrics, with the results being portrayed graphically using checkerboard plots as shown in Figure ES-1. In most regions and months, results showed more indicators of warming than of cooling – particularly as defined by the minimum temperature metrics. For example, an increase of  $\geq 0.5$  °F is observed in 55% of the grid cells in Figure ES-1 showing results of the 90<sup>th</sup> percentile 1-hr max. temperature, 81% of the grid cells showing 10<sup>th</sup> percentile 1-hr min. temperatures, and 86% of the grid cells showing 10<sup>th</sup> percentile 6-hr min. temperatures. Furthermore, the majority of these temperature changes are statistically significant at a 95% (or higher) confidence level.

The sign and magnitudes of the observed temperature changes are variable across the regions, months, and temperature metrics examined. Nevertheless, it can be seen from Figure ES-1 that increases in the 1-hr max. temperature values are smaller and less regionally extensive than increases

in the min. temperature values. Conversely, decreases in the 1-hr max. temperature values are larger and more regionally extensive than decreases in the min. temperature values. The 90<sup>th</sup> percentile 1-hr max. temperatures show widespread warming in March and widespread cooling in October. The 90<sup>th</sup> percentile 1-hr max. temperatures show less warming in summer compared to the remainder of the year. During the summer months of June through August, only two region-month combinations show warming in excess of 1.5 °F – Rocky Mountain in July and New England in August.

Differences in monthly 10<sup>th</sup> percentile min. and 90<sup>th</sup> percentile max. temperature values between the Doner and the Modern eras were also determined on a state-by-state basis. However, only 5 of the 50 states have 10 or more stations upon which to base such comparisons. Because of this and other limitations, paired t-test statistical analyses were not performed to assess state-specific temperature differences.

A more comprehensive analytical approach to define the spatial and temporal distributions of current ambient temperatures may be warranted. Such an approach could draw upon modern high-resolution datasets such as the Parameter Regression on Independent Slopes Model (PRISM) as well as a larger pool of station data, such as the Applied Climate Information System (ACIS). Using this modern approach would provide a more accurate depiction of temperature patterns – especially in areas of complex terrain – by utilizing a much larger number of weather stations. The recommended approach would increase the number of weather stations from 340 in the Doner Report to more than 10,000 in the ACIS database and more than 15,000 in the PRISM model. However, a limitation of these more extensive databases is their reliance on daily max. and min. temperatures, not hourly values. Because of this, 6-hr min. temperature values could not be determined from these larger datasets.

It is also recommended to adopt the 30-year climate normal period that is used by the World Meteorological Organization (WMO). This period is updated every 10 years, and is used as a benchmark for climate evaluations.

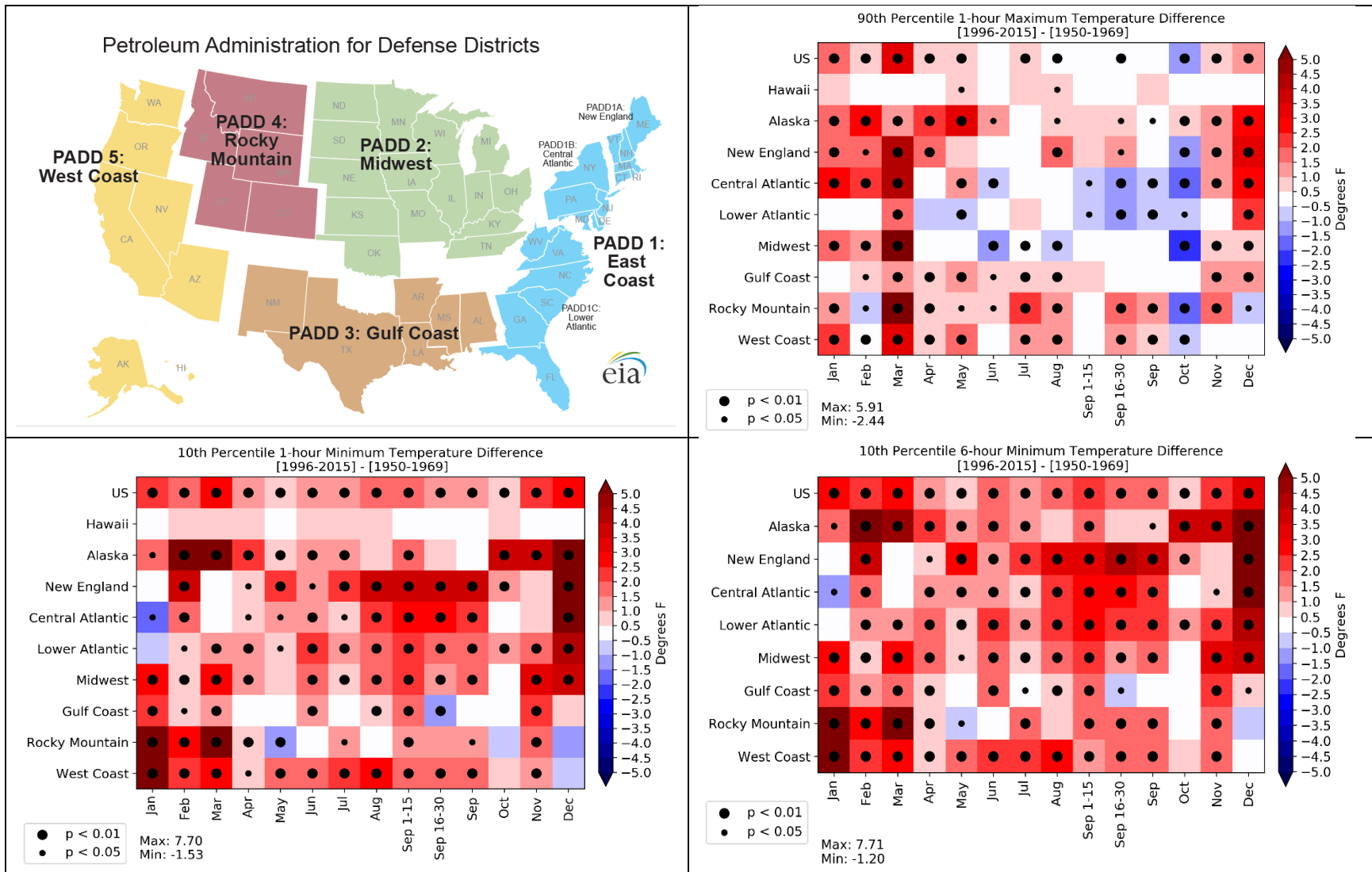


**Figure ES-1. Temperature differences between Doner Era (1950-1969) and Modern Era (1996-2015) by month and PADD**  
 (Note: “p” refers to the statistical p-value. For grid cells showing no dot,  $p > 0.05$ .)

## 2 Introduction and Background

U.S. Gasoline volatility specifications vary geographically and temporally to account for differing climatic conditions. The ASTM standard for automotive spark-ignition engine fuel (ASTM D4814) defines volatility classes for each state (or portion of a state) and each month – with two periods being used to designate the month of September (Sept. 1-15 and Sept. 16-30) to be consistent with EPA regulations regarding vapor pressure.<sup>1</sup> These volatility class designations are denoted by an alpha-numeric code that indicates both vapor pressure limits and vapor lock protection requirements. The alphabetic labels designating the six vapor pressure class requirements are shown in Table 1.

**Table 1. Vapor Pressure Class Requirements in ASTM D4814**

Class	AA	A	B	C	D	E
Max. vapor pressure at 100 °F, kPa (psi)	54 (7.8)	62 (9.0)	69 (10.0)	79 (11.5)	93 (13.5)	103 (15.0)

ASTM D4814 also defines six vapor lock protection classes, as shown in Table 2. These classes are defined by minimum temperatures at which the volume ratio of gasoline vapors to liquid gasoline (V/L) is equal to 20, when determined at ambient pressure. It has been found that vapor lock and other hot fuel handling problems are indicated by the temperature at which V/L = 20. As temperatures increase, the V/L ratio also increases for a given fuel. Thus, locations and times with warmer ambient temperatures have higher minimum temperature limits for V/L=20, while those with cooler ambient temperatures have lower minimum temperature limits.

**Table 2. Vapor Lock Protection Class Requirements in ASTM D4814**

Class	1	2	3	4	5	6
Min. temp. for V/L ratio of 20, °C (°F)	54 (129)	50 (122)	47 (116)	43 (107)	39 (102)	35 (95)

The ambient temperature data used to assign the volatility class designations in ASTM D4814 were taken originally from hourly weather information that was compiled and analyzed by the U.S. Army in the early 1970's. In particular, the 90<sup>th</sup> percentile 1-hr max. temperature values and the 10<sup>th</sup> percentile 6-hr min. temperature values for each month were used to define gasoline volatility classes for different areas. (The 6-hr min. temperature is defined as the highest temperature of the six coldest consecutive hourly temperature readings of a 24-hr day. This metric is used to represent the cold-soak temperature experienced by a vehicle.) These data, and the methodology by which they were analyzed, are documented in a 1972 report authored by John P. Doner, hence the name, "Doner Report."<sup>2</sup>

As an illustration of how these temperature data are used to assign alpha-numeric values for volatility classes, Table 3 shows the guidance offered in ASTM D4814 for making such designations in areas outside the U.S. For example, a designation of A-1 would be made for any month in a region where the 10<sup>th</sup> percentile 6-hour min. daily temperature exceeded 60 °F (16 °C) and the 90<sup>th</sup> percentile 1-hr max. daily temperature exceeded 110 °F (43 °C).

**Table 3. ASTM D4814 Guidance for Selecting Alpha-Numeric Designations for Gasoline Volatility**

Volatility Designation	10 <sup>th</sup> percentile 6-h min. Daily Temp., °C (°F)	90 <sup>th</sup> Percentile Max. 1-h Daily Temp., °C (°F)
A-1	>16 (60)	≥43 (110)
B-2	>10 (50)	<43 (110)
C-3	>4 (40)	<36 (97)
D-4	>-7 (20)	<29 (85)
E-5	≤-7 (20)	<21 (69)

In addition to gasoline volatility designations, temperature data from the Doner report are used to designate low temperature operability requirements for diesel fuel.<sup>3</sup> Table X5.1 in ASTM D975 lists the 10<sup>th</sup> percentile 1-hr min. temperature in each of 49 states (Hawaii is not included) for each of the six cold-weather months (October to March). For a few states (AK, AZ, CA, CO, FL, IL, NV, NM, NY, OR, PA, TX, and WA) separate values are given for different regions within the state.

### **2.1 Doner Methodology**

Temperature data utilized in the Doner report were acquired from 340 weather stations throughout the U.S. Most stations were located at airports or military facilities. The approximate period of record for 204 of these stations was 15 years (1950-1964), while a longer period of record (up to 21-years) existed for other stations. Although not strictly true for most of the 340 stations, it is sometimes stated that the Doner period of record was 21-years (1950-1970). However, as shown in the station listing (Appendix A-1 in the Doner Report), the actual periods of record used were quite inconsistent. Some station records began as early as 1948 (e.g., Trinidad, CO; Bridgeport, CT; Muskegon, MI) with others as late as 1960 (e.g., Fort Leonardwood, MO; Fort Hood, TX). In addition, some stations had gaps in their periods of record (e.g., Blytheville, AR; Moline, IL; Russell, KS; Victoria, TX; Wendover, UT).

To develop temperature distributions and percentiles, the Doner Report started with hourly weather station data and then developed daily max. and min. temperatures grouped into months. For example, using the 1950-1964 period of record, the January 1-hr max. and min. temperature distributions for a single station would each contain 465 records. For each day of the month (31 for January) and for each year (15) the max. and min. hourly temperatures were obtained and lumped into monthly distributions. Only days for which 24 individual hourly temperature readings were available were included. These temperature distributions were then used to determine specific percentile values assigned to each station for the purpose of generating isothermal maps for each month. The temperature percentile values were determined from cumulative frequency distribution plots developed from the 1-hr max. and 1-hr min. data for each station and month.

Appendix tables in the Doner Report contain monthly numerical summaries of these temperature distributions for each weather station. Only 12 monthly periods are included, as September was not divided into two parts by Doner. The division of September into two halves, as appears in the current gasoline volatility specifications of ASTM D4814, occurred later, in response to air quality regulations for volatile organic compounds (VOCs). For the 1-hr max. temperature distributions, values are provided for various percentile levels from 50% to 100%. For the 1-hr min. temperature

distributions, values are provided for various percentile levels between 0% to 50%. In addition, percentile values are presented for distributions of 3-hr min. and 6-hr min. temperatures.

Isothermal maps are presented in the Doner report for each month and for two metrics: 10<sup>th</sup> percentile 1-hr min. and 90<sup>th</sup> percentile 1-hr max. temperature. No maps are included that show 3-hr min. or 6-hr min. temperatures. The report contains no documentation on exactly how these maps were generated, or on the interpolation process used. Considering the statistical and plotting tools available at that time, it is likely that the isotherms in the Doner report were drawn manually.

## ***2.2 Project Objectives***

Because many years have passed since the Doner Report was issued, it is of interest to update that report with more recent meteorological data. Therefore, this study evaluated more modern ambient temperature data in a manner similar to that done in the Doner Report. Comparing monthly temperature data from the Modern era with those from the Doner era provides an indication of when (month), where, and how much the temperature has changed between the two time periods. While this study focused on determining the times and locations having significant temperature differences, it was not meant to examine the underlying meteorological records at specific weather stations, or to explain the reasons for the observed temperature differences.

In conducting this project, the intent was to replicate the original Doner methodology as closely as possible with respect to selection of weather stations and data processing methods, while using a more modern 20-year period of record (1996-2015) for comparison. In addition, a more modern approach was used to process and display the data, including portrayal of isothermal maps for both time periods. As in the Doner Report, we focused on data processing and display of three temperature metrics that are relevant with respect to gasoline and diesel fuel requirements: (1) 90<sup>th</sup> percentile 1-hr daily max., (2) 10<sup>th</sup> percentile 1-hr daily min., and (3) 10<sup>th</sup> percentile 6-hr daily min. Because the Doner report does not contain digitized data, we also applied this methodology to archived Doner era temperature data (1950-1969) to produce results in suitable formats for comparison with the Modern era data (1996-2015). In essence, the original Doner study was replicated twice, using archived temperature data from two time periods and a subset of the original stations.

## **3 Methodology**

### ***3.1 Selection of weather stations***

The Doner study included temperature data from a total of 340 weather stations. Nearly all of these stations were located in the contiguous U.S. (CONUS; 304 stations) and Alaska (34 stations), but 2 stations were in Panama. No stations were included from Hawaii. Although not explained in the Doner Report, Hawaii may have been excluded because, at that time, most Hawaii stations reported only daily max. and min. temperatures, but not individual 1-hr measurements. The complete list of Doner stations is provided in Appendix I-A, where it has been digitized and annotated with additional information.

Most of the Doner stations are located at airports and Air Force Bases. The Federal Aviation Administration (FAA) identification label is shown for each location, and the 4-digit International

Civil Aviation Organization (ICAO) identification is included in a few cases. Each station is also identified by its Weather Bureau Army Navy (WBAN) ID number. Use of these WBAN numbers makes it possible to obtain archived weather information from each station.

To supplement the Doner list of weather stations, 21 additional Hawaii stations were selected from a database maintained by NOAA's National Center for Environmental Information (NCEI). [Note: NOAA's NCEI was formerly known as the National Climatic Data Center (NCDC).] Most of these stations, however, do not include continuous 1-hr temperature data, but only daily max. and min. temperatures. Because of this limitation, it is not possible to evaluate 6-hr min. temperature data for Hawaii. Although the Doner study did not include any of these Hawaii stations, it is still possible to compare Modern and Doner era temperatures in Hawaii by accessing historical data from archived databases.

When analyzing temperature change signals over different time periods, there are several factors related to weather station location that should be considered. Most notable is the enhanced air temperature warming signal related to urbanization and population growth, known as the urban heat island (UHI) effect. Changes in land use and land cover driven by urban growth (i.e., more concrete and asphalt and less vegetation and bare soil) alter the land surface characteristics that control radiation and heat transfer through the atmospheric boundary layer. The UHI can cause accelerated warming in comparison to surrounding rural areas.<sup>4,5</sup> Most of the stations used in this study are located at airports that are in urban areas, and may therefore contain UHI signals in the temperature trends. To a certain degree, this study is comparing temperatures between a less developed time period (Doner era) and a more developed time period (Modern era). However, it should be noted that increasing air temperature is not restricted to urban areas. Many studies have also found amplified warming in remote mountain regions at higher elevations, a phenomenon known as elevation-dependent warming.<sup>6,7</sup> Analyses related to identifying the UHI influence (and other influences) on the temperature trends of weather stations used in this study are outside the scope of work.

### ***3.2 Acquisition of temperature data***

Although a large amount of temperature data was collected and processed as part of the original Doner study, that information is not available digitally. Therefore, it was decided to retrieve archived temperature data, both to replicate the analysis performed by Doner, and to conduct the same type of analysis using a more recent time period. The principal source of archived temperature data that was used is the Midwest Regional Climate Center (MRCC; <http://mrcc.isws.illinois.edu/CLIMATE/>). By referencing the WBAN ID numbers for the 338 CONUS plus Alaska weather stations used by Doner, hourly temperature data were requested for two 20-year time periods of interest: (1) Doner era (1950-1969) and (2) Modern era (1996-2015).

Through this process, it was discovered that the MRCC archived metadata did not include hourly temperature data for 35 of the 338 original Doner stations. About one-half of these 35 stations had been deactivated at some time between the Doner and Modern eras. For several of the other stations, it was possible to obtain the necessary 1-hr temperature data from NCEI. In total, temperature data covering at least parts of the Doner and Modern eras were located for 296 of the original 338 Doner stations. With addition of 21 Hawaii stations, this gave a total of 317 stations used in the current study. A graphical example of the type of data retrieved from the historical databases is provided in

Figure 1, which shows hourly temperatures recorded at the Eau Claire, WI weather station throughout the entire year of 1950.

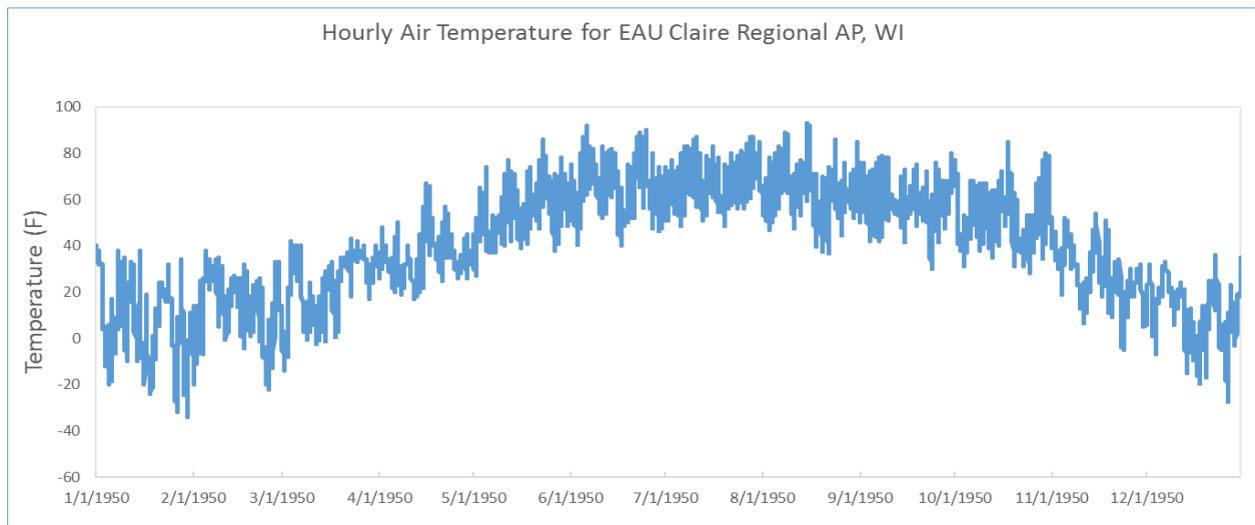


**Figure 1. Hourly temperature data from Eau Claire, WI (WBAN ID 14991) for 1950 generated using the MRCC’s cli-MATE tool (<http://mrcc.isws.illinois.edu/CLIMATE/>).**

### ***3.3 Data processing and acceptance criteria***

Several steps were taken to ensure acceptable quality of the raw temperature data prior to conducting further data analysis. First, the hourly temperature record for each station was inspected to identify missing values. For any given day, if a station reported fewer than 24 hourly values, the entire day was eliminated, and marked as missing data. This step was taken because the max. and min. temperatures could occur at any hour of the day, including an hour where no data were reported. This initial data quality procedure was not applied to the Hawaii stations, where only daily max. and min. temperatures were reported, not hourly values.

The hourly temperature records obtained for each station were analyzed to determine the 1-hr max., 1-hr min., and 6-hr min. values for each day. As was done in the Doner study, data from each station were lumped by month. Thus, the dataset for a given station includes several hundred data points per month, for each metric. For example, a complete dataset for a particular station (in either the Doner era or the Modern era) would include 620 observations for January – 31 days/month x 20 years.

Before further processing the collected data to determine monthly temperature distributions for each station and to identify various percentile values from these distributions, the extent of data completeness was examined. This was done for each station, month, and temperature metric. Percent data completeness was then calculated as the number of valid observations divided by the total possible number of observations. For example, a station with 500 valid January 1-hr max. observations would have a data completeness of  $500/620 \times 100 = 80.6\%$ .

Figure 2 shows the completeness of 1-hr max. temperature data in January for all 317 stations that had periods of record during both the Doner and Modern eras. [The x-axis numbering reflects the ordering of the stations as listed in Appendix I-A (with inclusion of Hawaii stations in their correct alphabetical location in the list).] Graphs for other months, and for 1-hr min. temperature data, are

similar. These graphs show that the degree of data completeness varies from station-to-station – during both time periods. The Doner era graph (top panel in Figure 2) shows a large number of stations having data completeness values near 75%. This is a consequence of the fact that around the year 1965, many stations switched from reporting 1-hr temperature data to reporting 3-hr data. Thus, for these stations, 1-hr data are not available for about 5 years of the 20-year Doner era. At some time before 1996, most of these stations again began reporting 1-hr data, so this 75% data completeness level is not as prominent in the Modern era graph (bottom panel of Figure 2).

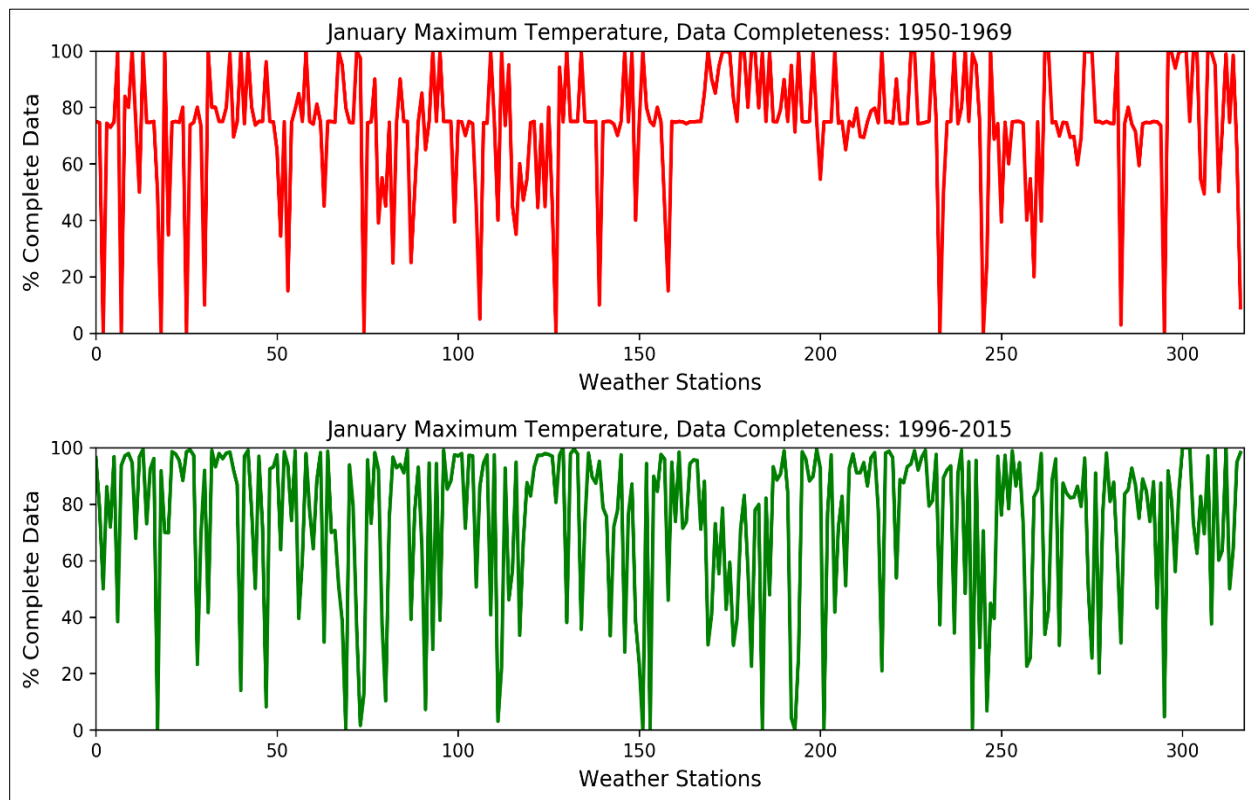


**Figure 2. Data completeness of January 1-hr max. temperature values from 317 weather stations recording data during the 20-year Doner era (top panel) and the 20-year Modern era (bottom panel).** (The 317 stations – ordered as shown in Appendix I-A, with addition of Hawaii – represent all stations having at least partial temperature records during both the Doner era and the Modern era.)

Figure 2 also shows that during both time periods, some stations stand out as having particularly low data completeness levels. In a few instances, these “outliers” come from the same stations during both periods, although there is not overall strong correspondence in these outlier stations between the two time periods. Based upon cursory examination of the data, it appears that stations having low percent data completeness had lengthy data gaps of months-to-years in duration, and did not simply have sporadic missing days. A more extensive examination (beyond the scope of this project) would be necessary to fully understand the reasons for data gaps from individual stations. Overall, data completeness for the 317 stations is similar in the Modern era as compared to the Doner era. Table 4 shows a comparison of data completeness by month for each of the three temperature metrics. (For the 6-hr daily min. metric, the Hawaii stations were not included in the assessment of data completeness.) Each value in Table 4 was computed as the mean of the percent data completion at all

stations for a given month and temperature metric (i.e., the January 1-hr max. value for the Doner era is the average of the red line in Figure 2).

**Table 4. Average Percent Data Completeness of Temperature Records from 317 Weather Stations**

	1-hr daily max.		1-hr daily min.		6-hr daily min.*	
	Doner	Modern	Doner	Modern	Doner	Modern
Jan	73.22	74.02	73.21	74.00	72.55	73.36
Feb	73.27	74.96	73.25	74.96	72.57	74.47
Mar	73.28	74.41	73.26	74.42	72.64	73.80
Apr	73.58	73.67	73.58	73.67	72.95	73.08
May	73.59	72.95	73.57	72.94	73.00	72.26
Jun	73.68	73.73	73.65	73.71	73.01	72.95
Jul	73.64	71.77	73.63	71.75	72.95	70.96
Aug	73.67	72.68	73.66	72.67	72.96	71.89
Sep	73.62	72.71	73.59	72.72	72.90	72.02
Oct	73.63	73.19	73.62	73.19	72.93	72.54
Nov	73.74	72.80	73.73	72.79	73.05	72.17
Dec	73.55	71.84	73.50	71.83	72.92	71.19
Average	73.54	73.23	73.52	73.22	72.87	72.56

\* Does not include Hawaii stations

When evaluating and comparing large meteorological datasets, it is advisable to select a data completeness threshold level, so that the analysis is not unduly influenced by a few, possibly non-representative values. In addition, comparisons should be restricted to stations that have substantial periods of record during both time periods of interest. The designation of a specific data completeness threshold level is somewhat arbitrary, depending upon the database in question and the types of analyses being conducted.

To provide guidance regarding selection of a specific threshold value in this study, an assessment was conducted to determine how many of the total 317 stations would be included if a range of different data completeness thresholds were applied. This showed that using a relatively high threshold value would eliminate a large number of stations, particularly during the Doner era. For example, applying an 80% data completeness threshold would retain 186 stations from the Modern era, but only 96 stations from the Doner era. (Note from Figure 2 that an 80% data completeness threshold would eliminate the large number of stations having data completeness levels near 75%.) Relaxing this threshold allows for inclusion of many more stations. In the extreme case, with no threshold value, all 317 stations would be included. However, this would grant equivalent data weighting to a station having just a few temperature measurements during a 20-year period as to a station having hundreds of measurements during the same period.

Based on this type of evaluation, a data completeness threshold of 50% was selected to provide a reasonable balance between maintaining a statistically and geographically robust dataset, and avoiding stations that may have non-representative data. Considering a 20-year time period, a 50% data completeness threshold ensures that only stations having at least 10-years of data (during both time periods) will be considered. Applying this 50% threshold results in about 220 stations being used to compare 1-hr max. and 1-hr min. temperatures, and about 200 stations being used to compare 6-hr min. temperatures. (Six-hour min. temperatures have fewer stations due to elimination of the

Hawaii stations. The exact numbers of stations used for each metric in each month are shown in Table 5.

**Table 5. Number of Stations (Satisfying 50% Data Completeness Threshold) used to Compare Temperature Data between the Doner and Modern Eras**

	1-hr max.	1-hr min.	6-hr min.*
Jan	219	219	201
Feb	224	224	206
Mar	222	222	204
Apr	220	220	202
May	218	218	201
Jun	218	218	201
Jul	217	216	200
Aug	218	218	200
Sep	218	218	201
Oct	219	219	202
Nov	216	216	201
Dec	217	217	200

\* Does not include Hawaii stations

All weather stations that met the 50% data completeness threshold for at least one specific month during both the Doner and Modern periods are listed in Appendix I-B. The locations of these 228 stations are shown on the map of Figure 3, which also highlights the regional areas defined as Petroleum Administration for Defense Districts (PADDs). The circled numbers in this figure indicate the number of stations in each PADD that were included in the analysis.

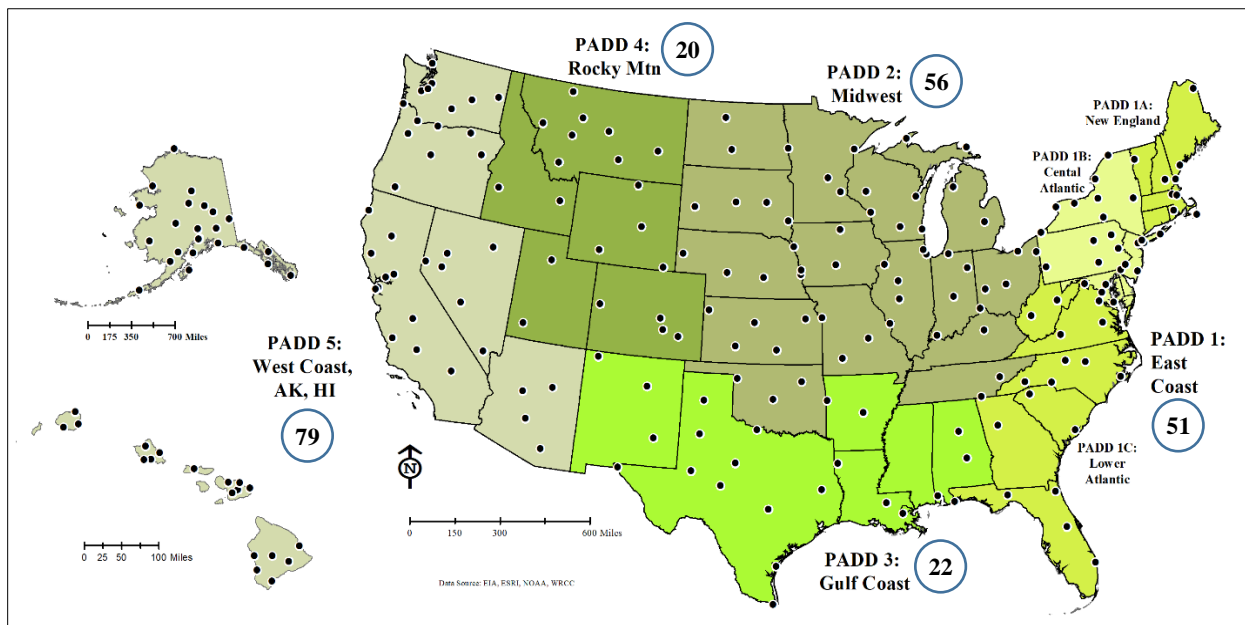


**Figure 3. Locations of the 228 weather stations used in this study. Numbers in circles indicate the number of stations in each PADD.**

### 3.4 Data analysis and display methods

Individual station data were batched, processed, and analyzed using the Python programming language. For each station and month that satisfied the 50% data completeness requirement, monthly percentile temperature values were determined (90<sup>th</sup> percentile 1-hr max., 10<sup>th</sup> percentile 1-hr min., and 10<sup>th</sup> percentile 6-hr min.) using cumulative frequency distributions, as was done by Doner. These values were determined for each complete month, as well as for Sept. 1-15 and Sept. 16-30, for both the Doner and Modern eras. All the computed percentile values are provided in Appendix II, as a set of 6 tables (3 temperature metrics x 2 time periods), as well as 3 additional tables showing the differences between the two time periods. The master dataset used to produce these tables was also used for all subsequent analysis, including comparisons made between the Doner and Modern eras.

Appendix Tables II-1, II-2, and II-3 provide the 90<sup>th</sup> percentile 1-hr max., 10<sup>th</sup> percentile 1-hr min., and 10<sup>th</sup> percentile 6-hr min. temperatures, respectively, for each station during the Doner era. Appendix Tables II-4, II-5, and II-6 provide the comparable temperature values during the Modern era. These appendix tables provide temperature data similar to what is included in Appendix A-2 of the Doner Report. It is these Doner data that were used to establish the gasoline volatility classifications included in ASTM D4814 and the diesel fuel low temperature requirements included in ASTM D975.

Monthly temperature results for each station and each metric were prepared as dot maps, with the color of the dot indicating the temperature value. These maps are included in Appendix III. Besides separate maps for the two periods, difference dot maps were also created to illustrate the station-by-station temperature differences between the two time periods. These difference maps are portrayed as the Modern era temperature minus the Doner era temperature. Thus, red colors in the difference dot maps indicate a warming trend since the Doner era, while blue colors indicate a cooling trend.

The same data for preparing dot maps was used to create interpolated temperature maps, in which different colors were used to represent temperature isotherms. This was done by spatially interpolating station data to a 25x25 km grid for CONUS and Alaska, and a 5x5 km grid for Hawaii, using an inverse distance weighting (IDW) method. Following this method, assigned values are calculated for grid points that do not contain actual station data, based on distance-weighted averages of nearby stations. This simple interpolation method assumes each measured point has a local influence that diminishes with distance.<sup>8</sup> It should be noted that IDW does not account for elevation changes throughout the grid. Monthly interpolated maps for all three temperature metrics during both time periods are included in Appendix IV, along with maps showing differences between the two time periods.

Temperature differences between the two time periods were also examined by creating histograms showing the numbers of stations having higher and lower temperatures in the Modern era compared to the Doner era. This was done for each temperature metric and each month using the entire dataset (for total U.S.) as well as by PADD. The PADD-specific histograms are included in Appendix V; the entire dataset histograms are included in the Results and Discussion section of this report.

To test for statistically significant temperature differences between the Doner and Modern eras, paired t-tests (two-sided) were conducted. The null hypothesis states that the two samples have

identical average values. For this study, a difference in average values was considered statistically significant to the 95<sup>th</sup> percentile confidence limit (null hypothesis rejected) when the probability value (p-value) was less than 0.05. This statistical analysis was conducted for each of the three temperature metrics and each monthly period. Besides comparing temperature differences for the overall dataset (entire U.S.), these t-tests were performed over smaller regions, as defined by the PADDs. Some PADDs, however, include more stations than other PADDs. For example, PADD 2 (Midwest) has 56 stations, while PADD 1A (New England) has only 9 stations. Consequently, the statistical robustness varies across the different PADDs.

Due to interest in examining temperature changes within individual states, average monthly values of the three temperature metrics were calculated on a state-by-state basis for each of the two time periods. These data are included in Appendix VI. It should be pointed out, however, that these state-specific data have significant limitations. For example, only 5 of the 50 states have 10 or more weather stations, while 24 states have 3 or fewer stations. Connecticut and Mississippi have no stations. Having so few stations raises questions of data representativeness. While a single point may be acceptable to represent the entire State of Delaware, New Hampshire, Rhode Island, or Vermont, this may not be true for Georgia. Also, it seems unlikely that the entire State of Tennessee can be represented adequately by two stations, both of which are located near the eastern border. Similarly, the large, mountainous states of Idaho and Utah are unlikely to be represented adequately by two stations located over 250 miles apart.

Due to issues such as these, no t-test statistical analyses were performed on the state-specific temperature data. Also because of these severe data limitations, readers should be cautious in comparing the state-specific results with results obtained from other information sources that utilize a much larger database – such as the NCEI tool called “*Climate at a Glance*,” which is available at <http://www.ncdc.noaa.gov/cag/>.

## **4 Results and Discussion**

Results from this study are summarized and discussed for each of the three temperature metrics analyzed. These results are presented in several ways, including dot maps (Appendix III), interpolated maps (Appendix IV), and histograms (Appendix V). Because the main objective of this study was to quantify temperature differences between the Doner and Modern eras, this discussion is focused on the temporal and spatial differences determined for each of the three temperature metrics.

Because the temperature differences varied from month-to-month, it was decided to focus here on just two months illustrating the extremes of these differences: (1) March, which shows a broad warming trend in both max. and min. temperatures at most locations, and (2) October, which shows cooling of max. temperatures and weak warming of min. temperatures at most locations between the Doner era and the Modern era.

Finally, for each of the three temperature metrics, results of the statistical analyses conducted to assess the magnitude and statistical significance of temperature differences between the two time periods are presented, both for the entire U.S. and for each individual PADD. These statistical results are summarized in both tabular and graphical form in the sections below.

## **4.1 90<sup>th</sup> Percentile 1-hr max. temperature**

The 90<sup>th</sup> percentile 1-hr max. temperature results for the Doner and Modern eras are presented and compared below, using several visual and tabular tools.

### **4.1.1 Dot maps and interpolated maps**

Dot maps illustrating 90<sup>th</sup> percentile 1-hr max. temperatures for each station and month during both time periods are shown in Appendix III-A. In these appendix figures, each page consists of three map panels: the left panel shows temperatures during the Doner era, the middle panel shows temperatures during the Modern era, and the right panel shows temperature differences between the two time periods, expressed as Modern era minus Doner era. These difference dot maps (right panel) are the most relevant in addressing the objectives of the study as they portray the warming or cooling trends observed at each station.

In looking at all 14 time periods of the Appendix III-A figures side-by-side, differences between Doner and Modern era 90<sup>th</sup> percentile 1-hr max. temperatures clearly vary month-to-month. An overall warming trend is apparent, as the difference maps show more red dots than blue dots. This pattern, however, is not uniform either spatially or temporally. Two months which illustrate the extremes are shown in Figure 4. In March, warming is seen throughout the entire U.S., with the largest temperature increases occurring in the upper Midwest and portions of the Northern Plains, and the smallest increases occurring in eastern parts of Texas and along the Gulf Coast. In October, cooling is seen throughout most of the U.S., especially in the Northern and Central Plains. In contrast, Alaska shows either warming or no change during both March and October. Similar comparative analyses can be made for each month.

Another way to visualize these results is by means of color-coded interpolated maps, as shown in Appendix IV-A. These maps are based on the same data as used to produce the dot maps, but they make it easier to visualize the broader spatial patterns showing warming or cooling trends. The interpolated maps for the two extreme months of March and October are shown in Figure 5.

### **4.1.2 Histograms**

Another way to examine temperature differences between the Doner era and the Modern era is through use of histograms, which illustrate the number of weather stations exhibiting warming and cooling trends. Histograms were developed for each PADD (with Alaska and Hawaii treated separately) as well as for the entire U.S. In these histograms, temperature differences are binned into increments of 1°F, except for a double-wide bin from -1°F (blue line) to +1°F (red line). This special bin contains all the stations that showed no temperature differences between the two time periods. In many cases, this “zero bin” contained the largest number of stations. Without this special bin designation, temperature difference values of zero might otherwise be included in the 0 to -1 bin or the 0 to +1 bin, thereby presenting a skewed distribution. In each histogram, the double-wide zero bin is bracketed by blue and red vertical lines. Bins to the left of the blue line indicate cooler temperatures in the Modern era, while bins to the right of the red line indicate warmer temperatures in the modern era. The PADD-specific histograms are provided in Appendix V-A, with a separate figure included for each month. Histograms for the entire U.S. are shown in Figure 6, with a separate chart for each month.

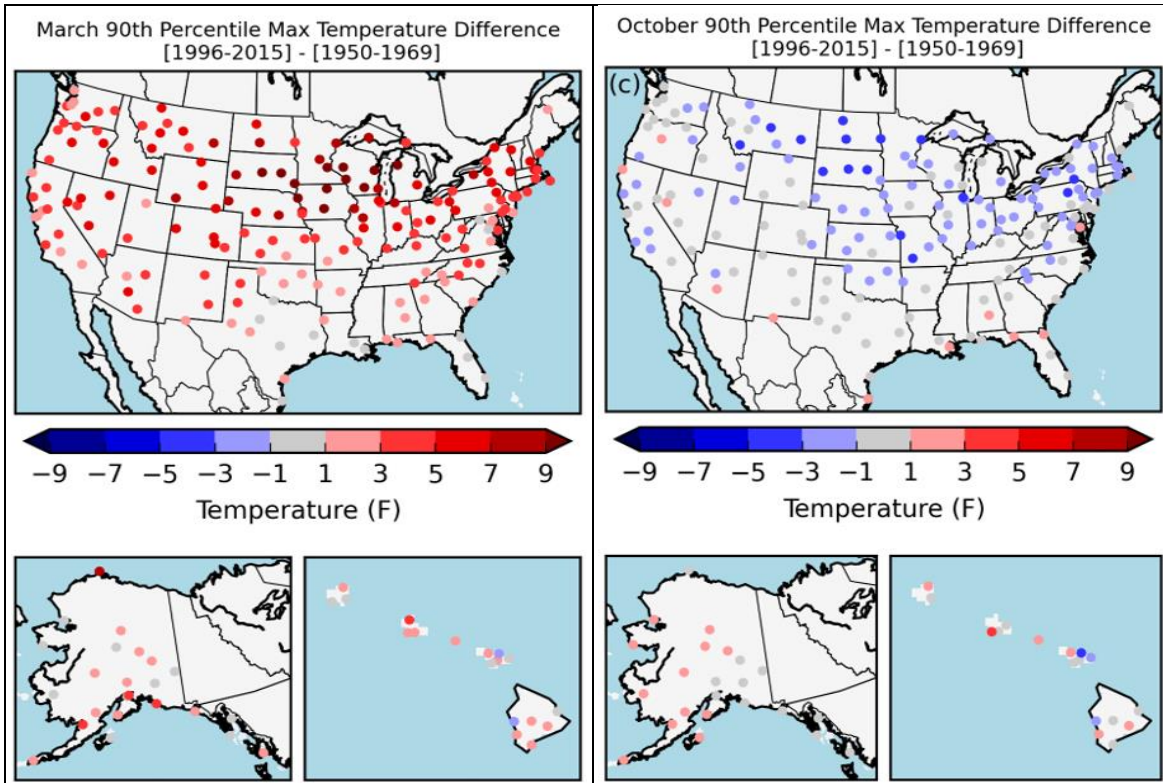


Figure 4. Dot maps showing differences in 90<sup>th</sup> percentile 1-hr max. temperature between Doner and Modern eras during March (left) and October (right).

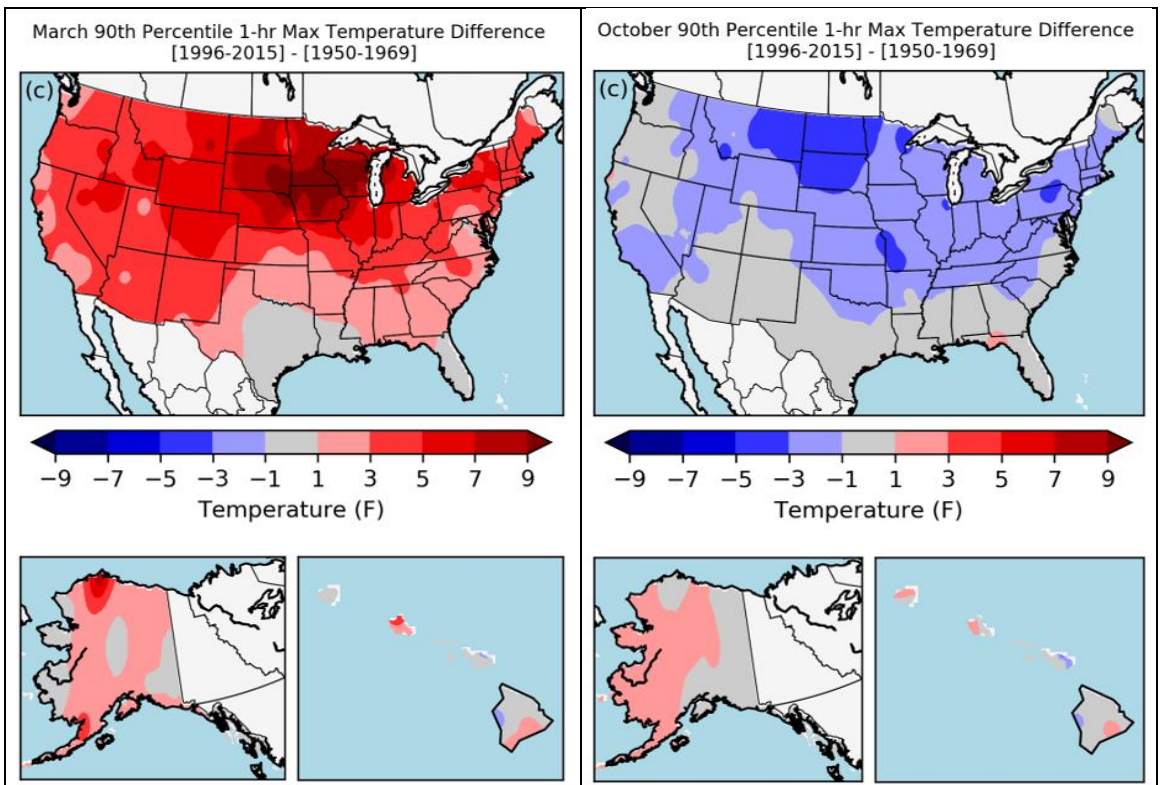
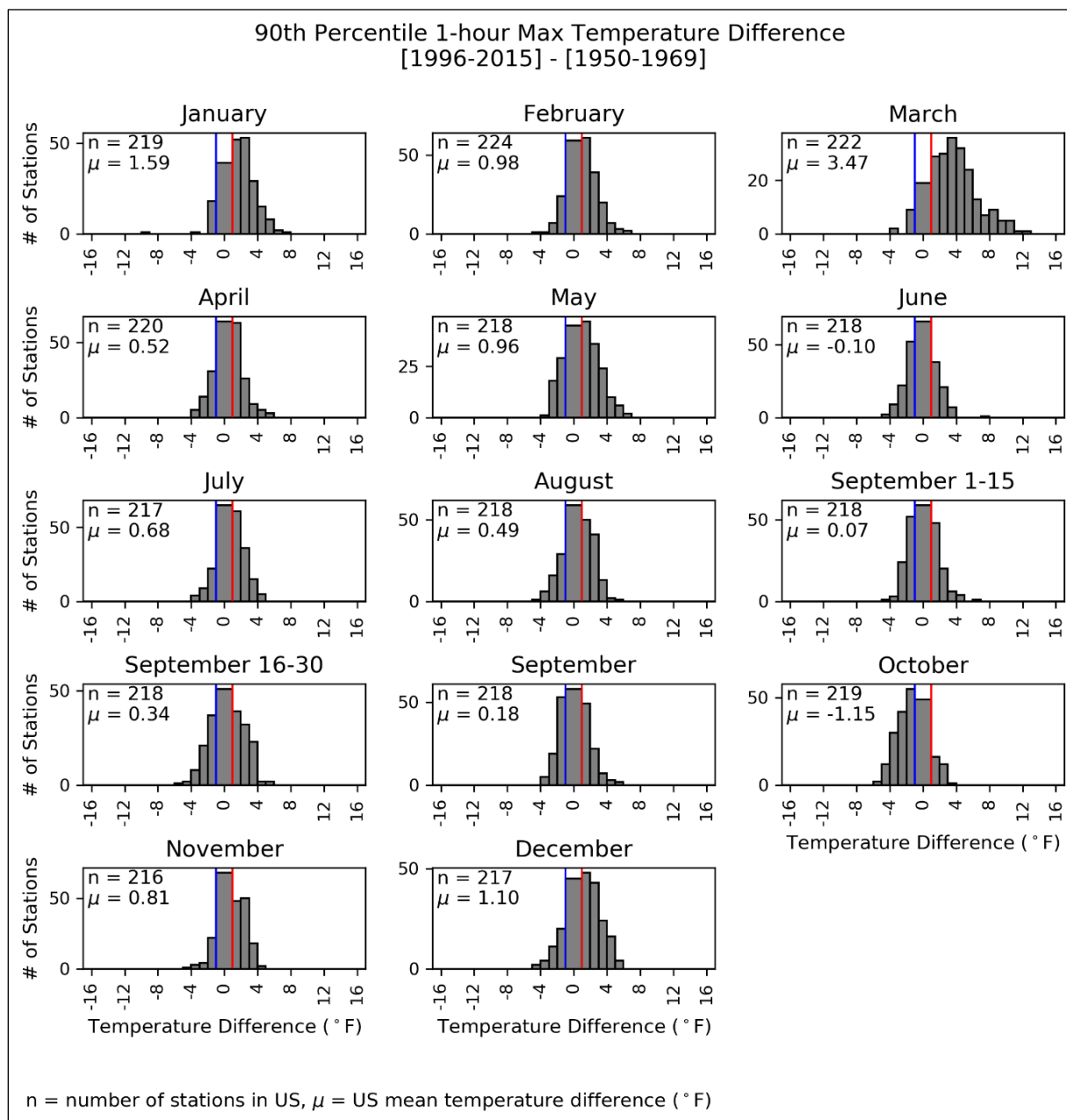


Figure 5. Interpolated maps showing differences in 90<sup>th</sup> percentile 1-hr max. temperature between Doner and Modern eras during March (left) and October (right).

The greatest temperature changes occurred in March and October, and are shown in Figure 6. In March, approximately 85% of the 222 stations have higher 90<sup>th</sup> percentile 1-hr max. temperatures in the Modern era as compared to the Doner era, with approximately 10% of the stations showing temperature differences between -1.0 °F and +1.0 °F, and less than 5% of the stations showing cooler temperatures of at least 1.0 °F. The overall average temperature change of all 222 stations is 3.47 °F. In October, approximately 10% of the stations have higher modern temperatures, while 20% have no temperature change greater than 1.0 °F, and 70% of stations had cooler temperatures. Overall, the average temperature change of all 219 stations in October was -1.15°F.



**Figure 6. Numbers of weather stations throughout the U.S. showing differences in 90<sup>th</sup> percentile 1-hr max. temperature between the Doner and Modern eras (by month).**

As suggested by the dot maps (Figure 4) and the interpolated maps (Figure 5) shown above, temperature histograms for March and October also show large regional variability. For example, Appendix Figure V-A-3 shows that in March, every station in the PADD regions of New England, Central Atlantic, Midwest, Rocky Mountain, and the West Coast experienced a warming trend, while stations in Alaska, Hawaii, Lower Atlantic, and the Gulf Coast exhibited mixed results. As seen in Figure 6, the histograms for all other monthly periods show relatively more normal distributions around zero. The average temperature difference of all stations, however, is positive (i.e., warming) for 12 of the 14 time periods shown. June and October are the only exceptions, showing overall cooling.

### 4.1.3 Statistical analysis of temperature differences

Differences between the 90<sup>th</sup> percentile 1-hr max. temperatures in the Doner and the Modern eras were analyzed statistically by month and PADD region (with Alaska and Hawaii being considered separately). The temperature differences between these two time periods, and the probability values (p-values) of the differences are given in Table 6.

**Table 6. Differences and associated p-values in 90<sup>th</sup> percentile 1-hr max. temperature between Doner and Modern eras (Modern – Doner)**

	US		HI		AK		New England PADD 1A		Central Atlantic PADD 1B		Lower Atlantic PADD 1C		Midwest PADD 2		Gulf Coast PADD 3		Rocky Mountain PADD 4		West Coast PADD 5	
	°F	p	°F	p	°F	p	°F	p	°F	p	°F	p	°F	p	°F	p	°F	p	°F	p
Jan	1.59	0.00	0.71	0.07	1.77	0.01	1.57	0.00	2.98	0.00	0.48	0.06	1.92	0.00	0.40	0.12	1.33	0.00	2.18	0.00
Feb	0.98	0.00	0.27	0.54	2.56	0.00	1.52	0.02	2.02	0.00	0.35	0.09	1.25	0.00	0.78	0.03	-0.52	0.02	0.47	0.01
Mar	3.47	0.00	0.44	0.30	1.31	0.00	4.03	0.00	4.04	0.00	1.69	0.00	5.91	0.00	1.40	0.00	5.04	0.00	3.40	0.00
Apr	0.52	0.00	0.37	0.38	2.37	0.00	1.86	0.01	0.47	0.11	-0.67	0.05	-0.16	0.42	0.56	0.01	0.82	0.00	0.65	0.00
May	0.96	0.00	0.96	0.03	3.24	0.00	0.54	0.31	1.42	0.00	-0.77	0.01	-0.04	0.66	1.19	0.01	0.92	0.02	1.81	0.00
Jun	-0.10	0.36	0.05	0.90	1.00	0.02	-0.38	0.20	-0.56	0.00	0.00	0.99	-1.30	0.00	0.75	0.03	0.67	0.04	0.28	0.18
Jul	0.68	0.00	0.66	0.17	-0.44	0.17	0.38	0.40	0.15	0.55	0.54	0.10	0.49	0.00	0.89	0.00	2.10	0.00	1.28	0.00
Aug	0.49	0.00	0.98	0.04	0.67	0.02	1.50	0.01	0.20	0.44	0.26	0.35	-0.71	0.00	0.96	0.00	1.33	0.00	1.35	0.00
Sep 1-15	0.07	0.54	0.41	0.31	0.61	0.19	0.50	0.19	-0.76	0.01	-0.62	0.02	-0.31	0.24	0.54	0.07	0.37	0.28	0.39	0.10
Sep 16-30	0.34	0.01	0.41	0.28	0.89	0.02	1.28	0.01	-1.06	0.00	-1.11	0.00	-0.04	0.95	0.03	0.91	1.90	0.00	1.24	0.00
Sep	0.18	0.09	0.89	0.35	0.34	0.04	0.36	0.30	-0.94	0.00	-0.60	0.01	-0.16	0.53	0.23	0.34	1.02	0.00	0.72	0.00
Oct	-1.15	0.00	0.05	0.90	0.73	0.00	-1.50	0.01	-1.96	0.00	-0.73	0.02	-2.44	0.00	-0.22	0.23	-1.87	0.00	-0.74	0.00
Nov	0.81	0.00	-0.20	0.64	1.08	0.00	1.13	0.01	1.04	0.00	0.34	0.27	0.93	0.00	1.09	0.00	1.66	0.00	0.21	0.38
Dec	1.10	0.00	0.35	0.39	2.78	0.00	3.05	0.00	2.79	0.00	2.12	0.00	0.92	0.00	1.10	0.00	-0.87	0.02	-0.41	0.11

Notes: Red-shaded cells indicate temperature warming of  $\geq 1.00$  °F (47 cells)  
 Blue-shaded cells indicate temperature cooling of  $\geq 1.00$  °F (8 cells)  
 Due to rounding, p-values shown as "0.00" indicate the values were  $<0.01$

Table 6 also highlights the months and locations showing warming trends of  $\geq 1.00$  °F (red color) and those showing cooling trends of  $\geq 1.00$  °F (blue color). A cursory look at these color shadings indicates approximately 6 times as many warming values as cooling values. Furthermore, all 55 of the highlighted temperature differences shown in Table 6 are significant to a 95% confidence level (p-value of  $< 0.05$ ), with 52 of the 55 being significant to a 99% confidence level (p-value of  $< 0.01$ ).

Of all the geographic regions considered, only Hawaii shows no significant temperature changes greater than 1.00 °F.

Another way to depict these temperature differences and their statistical significance is by a checkerboard plot, as shown in Figure 7. This figure shows the same information as in Table 6, but in an easier to visualize form. The color shading increments in Figure 7 are 0.5 °F, whereas the histogram increments shown in Figure 6 are 1.0 °F. This is simply a matter of convenience to improve the visual appearance of the histograms.

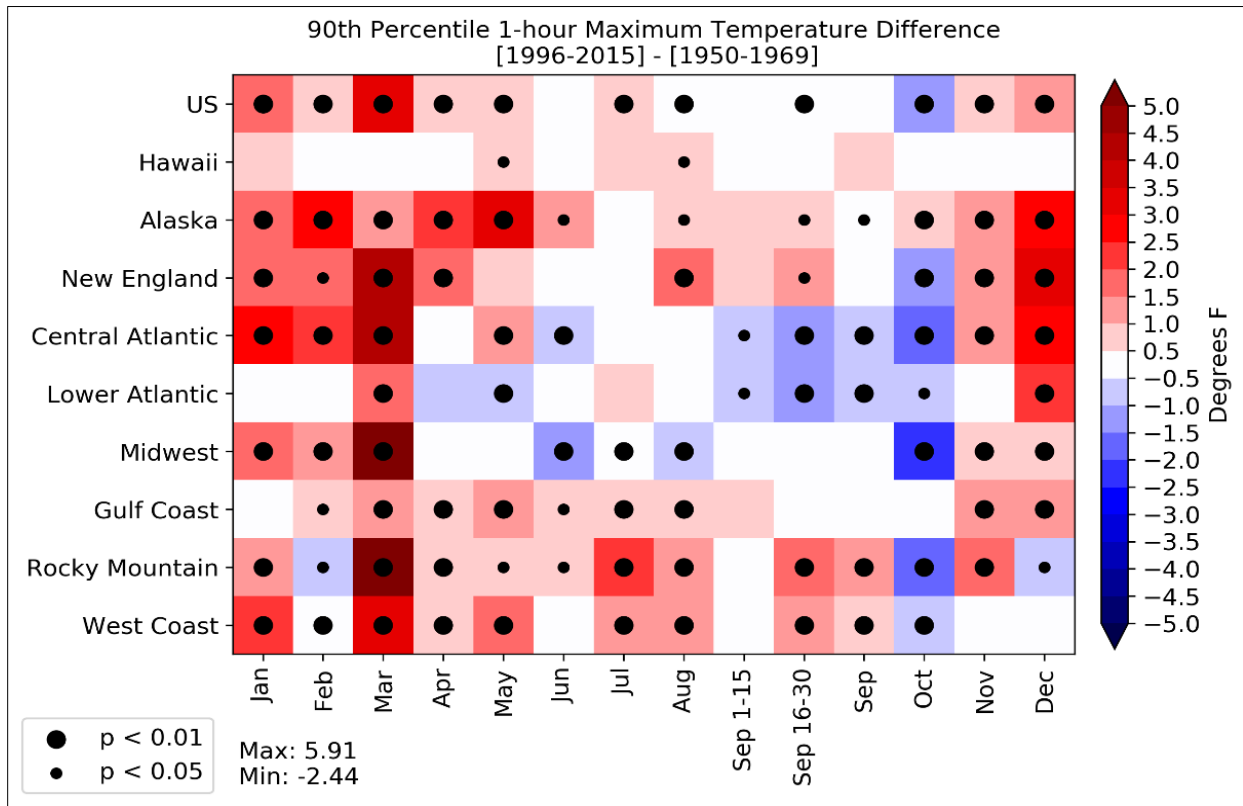


**Figure 7. Magnitude and significance of 90<sup>th</sup> percentile 1-hr max. temperature differences between the Doner era (1950-1969) and the Modern era (1996-2015) - by month and PADD.** (Note: “p” refers to the statistical p-value. For grid cells showing no dot, p > 0.05.)

The largest warming value in Figure 7 is 5.91 °F, which appears in PADD 2 (Midwest) in March. The largest cooling value is -2.44 °F, which also appears in PADD 2 in October. The white-colored grid cells in Figure 7 indicate temperature changes that fall between -0.5 and +0.5 °F. Even though these temperature changes are small, they can still be statistically significant, especially if they relate to a PADD with many stations. For example, the West Coast (PADD 5) temperature difference value in February is 0.47 °F, which is just below the 0.50 °F value to be shaded. This value was derived from analysis of 33 stations in PADD 5.

## **4.2 10<sup>th</sup> Percentile 1-hr min. temperature**

The 10<sup>th</sup> percentile 1-hr min. temperature results from the Doner and the Modern eras are presented and compared below, using the same visual and tabular tools as described above for the 90<sup>th</sup> percentile 1-hr max. temperature results.

### **4.2.1 Dot maps and interpolated maps**

Dot maps illustrating the 10<sup>th</sup> percentile 1-hr min. temperatures for each station and month during both time periods are shown in Appendix III-B. In looking at the 14 monthly periods analyzed, differences between the Doner and the Modern eras (right-hand panels of each figure in Appendix III-B) vary from month-to-month. As with the 90<sup>th</sup> percentile 1-hr max. temperatures, these min. temperature results also indicate a general warming trend in most locations and most times, showing more red points than blue points. The greatest differences between the Doner and the Modern eras occurred in March and October, and are presented in Figure 8. These 1-hr min. temperature values show the greatest warming in the Midwest and Rocky Mountain regions during March, and the greatest cooling (or least warming) in many of the same areas during October. Assessments of other months lead to different conclusions than for March and October. Of note is that regardless of month chosen, nearly all Alaska stations show warming trends.

Interpolation maps for the 10<sup>th</sup> percentile 1-hr min. temperatures from both the Doner and Modern eras are presented in Appendix IV-B. Results for each monthly period are presented as a separate page. Examples of difference interpolation maps for March and October are shown in Figure 9. March shows a widespread warming trend over much of the U.S., as do January and December, though these months are not shown here. Also, the month of October shows either a slight cooling trend or no warming throughout much of the central part of the country, with a similar trend being seen during the month of May.

### **4.2.2 Histograms**

Histograms showing the numbers of stations exhibiting warming and cooling trends with respect to the 10<sup>th</sup> percentile 1-hr min. temperature are provided in Appendix V-B. A separate page is included for each month, with histograms shown for each of the nine geographical regions being considered. A histogram depicting all stations throughout the U.S. is given in Figure 10.

Consistent with all trends observed in the dot maps (Appendix III-B) and the interpolated temperature maps (Appendix IV-B), the histograms in Figure 10 indicate that January, March, and December show the largest overall temperature increases between the Doner and the Modern eras, while May and October show the smallest overall temperature increases. The histograms in Appendix V-B, however, show a regional variation with the temperature change trends. For example, in the month of December, which has the overall highest temperature increase, every station in PADD 1 (New England, Central Atlantic, and Lower Atlantic) shows a warming trend, whereas more stations show cooling than warming in the Rocky Mountain and West Coast regions. In the month of October, which has nearly the smallest overall temperature increase, most stations in the Rocky Mountain region show a cooling trend, while most stations in Alaska show strong warming trends. For all 14 time periods, the mean temperature difference was positive, consistent with an overall warming signal in the Modern era compared to the Doner era.

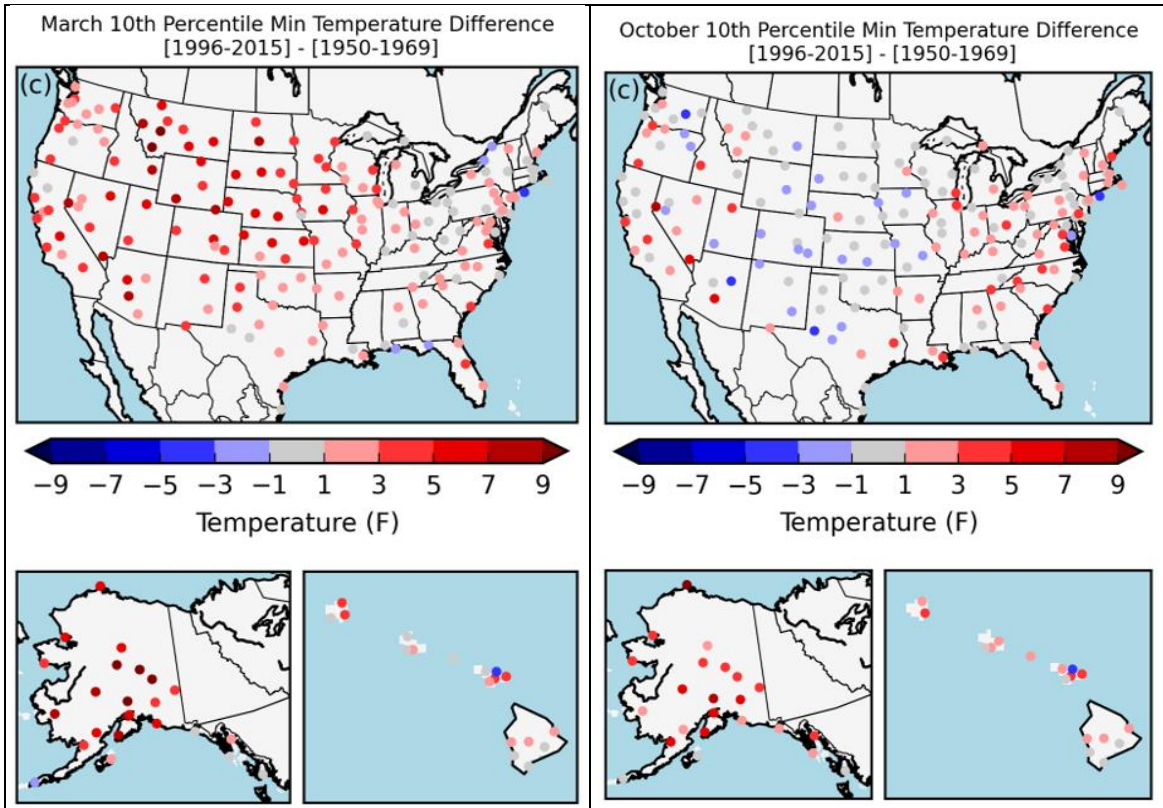


Figure 8. Dot maps showing differences in 10<sup>th</sup> percentile 1-hr min. temperature between Doner and Modern eras during March (left) and October (right).

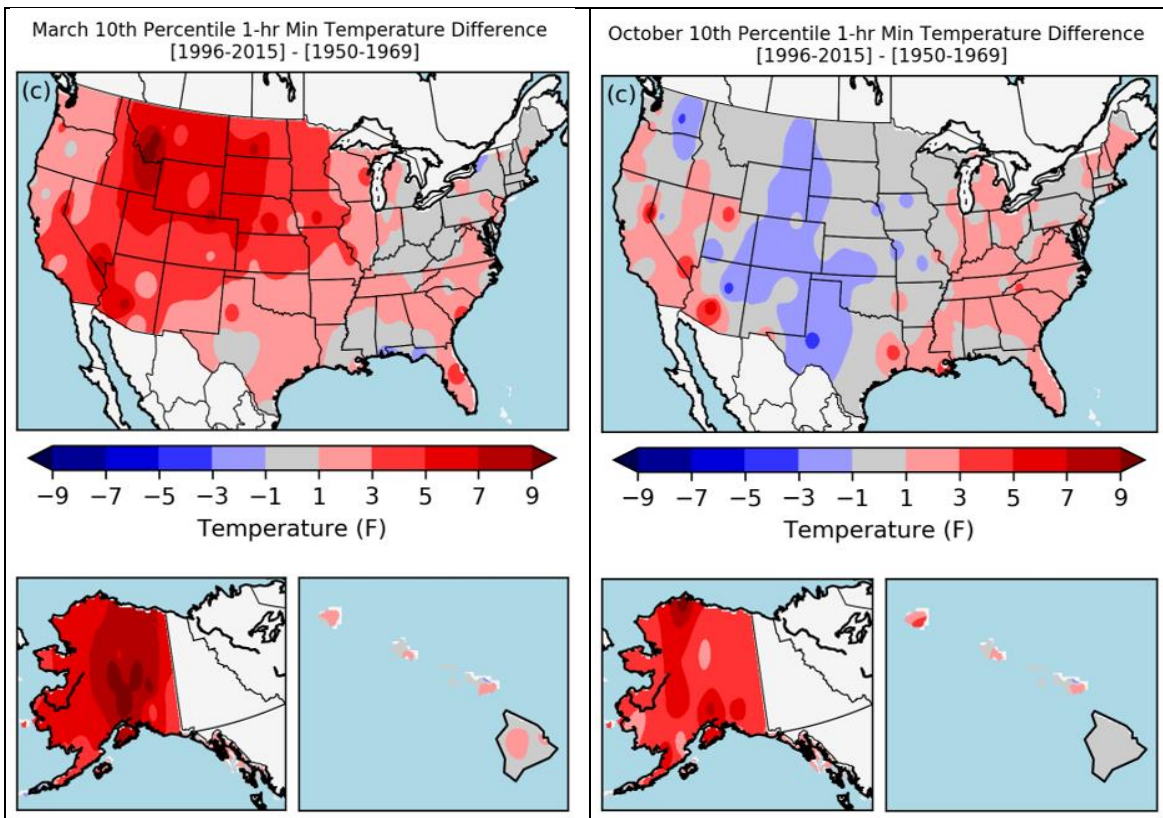
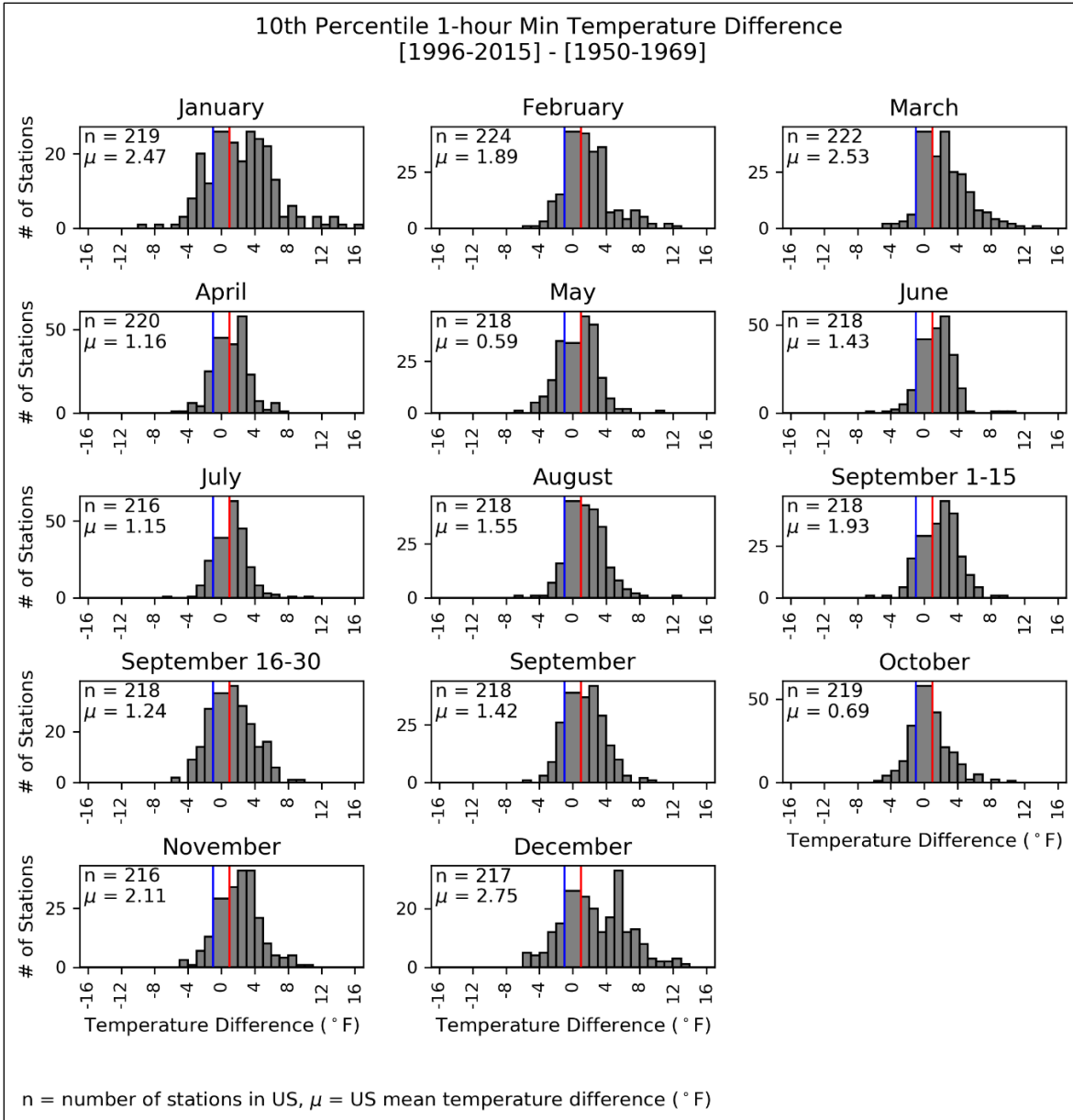


Figure 9. Interpolated maps showing differences in 10<sup>th</sup> percentile 1-hr min. temperature between Doner and Modern eras during March (left) and October (right).



**Figure 10. Numbers of weather stations throughout the U.S. showing differences in 10<sup>th</sup> percentile 1-hr min. temperature between the Doner and Modern eras (by month).**

### 4.2.3 Statistical analysis of temperature differences

Differences between the 10<sup>th</sup> percentile 1-hr min. temperatures in the Doner and the Modern eras were analyzed statistically by month and geographic region. These differences, and their probability values (p-values) are given in Table 7. In this table, locations and months showing a warming trend of at least 1.00 °F are highlighted in red, while locations and months showing a cooling trend of at least 1.00 °F are highlighted in blue. The results show far more instances of warming (85) than of cooling (4). Of the 89 highlighted temperature differences shown in Table 7, 87 are statistically significant to the 95% confidence level and 82 are statistically significant to the 99% confidence level. Of all the geographic regions considered, only Hawaii show no statistically significant temperature differences greater than 1.00 °F at the 95% confidence level.

**Table 7. Differences and associated p-values in 10<sup>th</sup> percentile 1-hr min. temperature between Doner and Modern eras (Modern – Doner)**

	US		HI		AK		New England PADD 1A		Central Atlantic PADD 1B		Lower Atlantic PADD 1C		Midwest PADD 2		Gulf Coast PADD 3		Rocky Mountain PADD 4		West Coast PADD 5	
	°F	p	°F	p	°F	p	°F	p	°F	p	°F	p	°F	p	°F	p	°F	p	°F	p
Jan	2.47	0.00	0.15	0.76	1.91	0.03	-0.49	0.31	-1.54	0.01	-0.64	0.56	2.95	0.00	2.21	0.00	7.02	0.00	5.47	0.00
Feb	1.89	0.00	0.56	0.32	5.87	0.00	3.77	0.00	1.75	0.00	0.91	0.02	0.68	0.00	0.74	0.03	2.51	0.00	2.09	0.00
Mar	2.53	0.00	0.73	0.11	5.18	0.00	0.33	0.45	0.20	0.60	1.14	0.01	2.67	0.00	1.37	0.00	5.51	0.00	2.84	0.00
Apr	1.16	0.00	0.67	0.17	2.34	0.00	0.78	0.04	0.88	0.05	1.39	0.00	1.47	0.00	0.37	0.29	0.72	0.01	0.89	0.03
May	0.59	0.00	0.12	0.82	0.98	0.00	2.35	0.01	1.04	0.03	0.76	0.02	0.50	0.09	-0.27	0.46	-1.38	0.00	1.64	0.00
Jun	1.43	0.00	0.85	0.12	1.49	0.00	1.41	0.05	1.26	0.00	2.25	0.00	1.55	0.00	1.42	0.00	-0.12	0.77	1.99	0.00
Jul	1.15	0.00	0.63	0.28	1.47	0.00	2.25	0.00	0.77	0.03	1.25	0.00	0.74	0.00	0.24	0.42	1.38	0.02	2.12	0.00
Aug	1.55	0.00	0.56	0.24	0.64	0.09	3.50	0.00	2.30	0.00	1.90	0.00	1.50	0.00	0.76	0.00	0.30	0.60	2.78	0.00
Sep 1-15	1.93	0.00	0.26	0.62	1.67	0.00	3.50	0.00	2.58	0.00	2.36	0.00	2.22	0.00	1.90	0.00	1.40	0.00	1.59	0.00
Sep 16-30	1.24	0.00	0.26	0.57	0.61	0.12	3.89	0.00	2.84	0.00	1.51	0.00	1.16	0.00	-1.07	0.00	1.20	0.07	1.76	0.00
Sep	1.42	0.00	0.48	0.46	0.35	0.17	3.88	0.00	2.45	0.00	1.85	0.00	1.59	0.00	0.15	0.57	1.36	0.02	1.73	0.00
Oct	0.69	0.00	0.71	0.15	3.75	0.00	1.48	0.00	0.00	0.99	1.24	0.00	0.11	0.59	-0.01	0.98	-0.57	0.20	0.62	0.19
Nov	2.11	0.00	0.27	0.62	3.73	0.00	0.60	0.14	0.70	0.09	1.97	0.00	3.22	0.00	2.05	0.00	1.63	0.00	1.44	0.01
Dec	2.75	0.00	0.35	0.45	7.70	0.00	6.41	0.00	5.30	0.00	4.26	0.00	3.58	0.00	0.62	0.11	-1.09	0.06	-0.55	0.21

Notes: Red-shaded cells indicate temperature warming of ≥ 1.00 °F (85 cells)  
 Blue-shaded cells indicate temperature cooling of ≥ 1.00 °F (4 cells)  
 Due to rounding, p-values shown as “0.00” indicate the values are <0.01

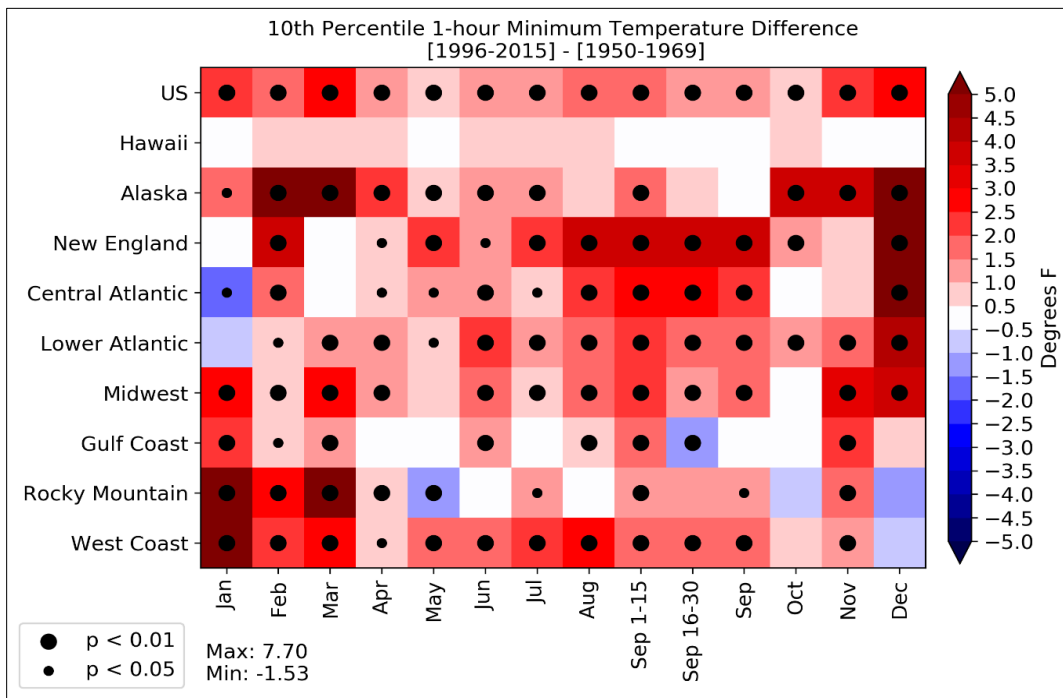


**Figure 11. Magnitude and significance of 10<sup>th</sup> percentile 1-hr min. temperature differences between the Doner era (1950-1969) and the Modern era (1996-2015) - by month and PADD.**  
 (Note: “p” refers to the statistical p-value. For grid cells showing no dot, p > 0.05.)

The checkerboard plot of Figure 11 provides a visual depiction of these statistical analyses. The single largest temperature increase of 7.70 °F is seen in Alaska in December, while the largest temperature decrease of -1.53 °F is seen in PADD 1B (Central Atlantic) in January. Figure 11 also indicates that the overall U.S. shows modest, but statistically significant to the 99% confidence level warming between the Doner and the Modern eras in every month. Several regions, including Alaska, New England, Rocky Mountains, and West Coast show very strong warming (> 5.0 °F) in a few months. Statistically significant cooling was observed in the Central Atlantic region during January, in the Rocky Mountain region during May, and in the Gulf Coast region during September 16-30. The latter two are at the 99% confidence level, while the first instance is significant to the 95% confidence level.

### **4.3 10<sup>th</sup> Percentile 6-hr min. temperature**

The 10th percentile 6-hr min. temperature results from the Doner and the Modern eras are presented and compared below, using the same visual and tabular tools as described above for the 90<sup>th</sup> percentile 1-hr max. temperature and 10<sup>th</sup> percentile 1-hr min. temperature results. Because the Hawaii weather stations did not report 1-hr measurements, computing the 10<sup>th</sup> percentile 6-hr min. temperature values for these stations was not possible. Thus, the results presented and discussed in this section do not include Hawaii.

#### **4.3.1 Dot maps and interpolated maps**

Dot maps illustrating the 10<sup>th</sup> percentile 6-hr min. temperatures for each station and month during both time periods are shown in Appendix III-C. As with the other temperature metrics, differences in the 10<sup>th</sup> percentile 6-hr min. values between the Doner and the Modern eras varied from month-to-month. The overall patterns of these temperature changes are similar to those seen for the 10<sup>th</sup> percentile 1-hr min. temperatures. The dot maps for March and October are shown in Figure 12, and the interpolated temperature maps are shown in Figure 13. Close inspection of these maps shows they are nearly indistinguishable from the dot maps and interpolated maps of the 10<sup>th</sup> percentile 1-hr min. temperatures (Figure 8 and Figure 9, respectively).

The temperature interpolated maps for all months are given in Appendix IV-C. Inspection of these appendix figures confirms that March shows widespread warming over much of the U.S., but the same trend is true for several other months, especially January and December. Also, the interpolated temperature maps confirm that the month of October shows a cooling trend (or no temperature change) over much of the central portion of the country (portions of PADDs 3 and 4), with a similar pattern being seen in May. These months showing the greatest changes in the 10<sup>th</sup> percentile 6-hr min. temperatures are largely consistent with the months showing the largest changes with respect to the 10<sup>th</sup> percentile 1-hr min. temperature metric.

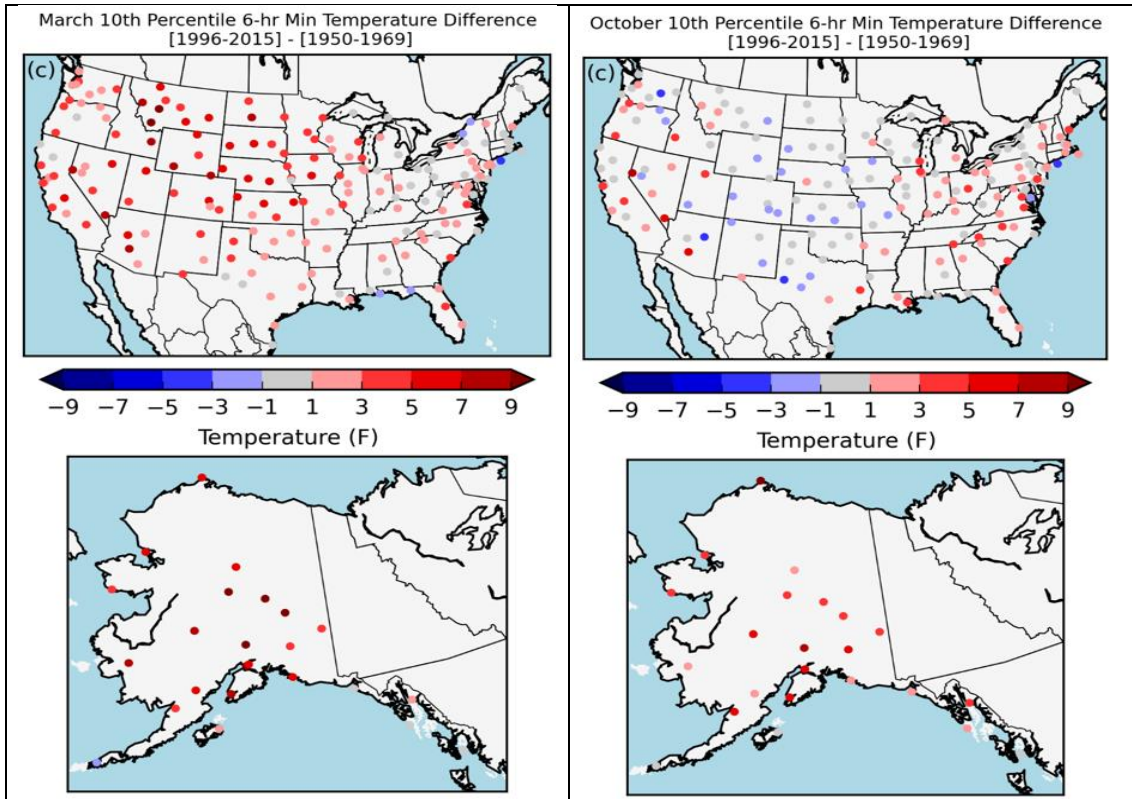


Figure 12. Dot maps showing differences in 10<sup>th</sup> percentile 6-hr min. temperature between Doner and Modern eras during March (left) and October (right).

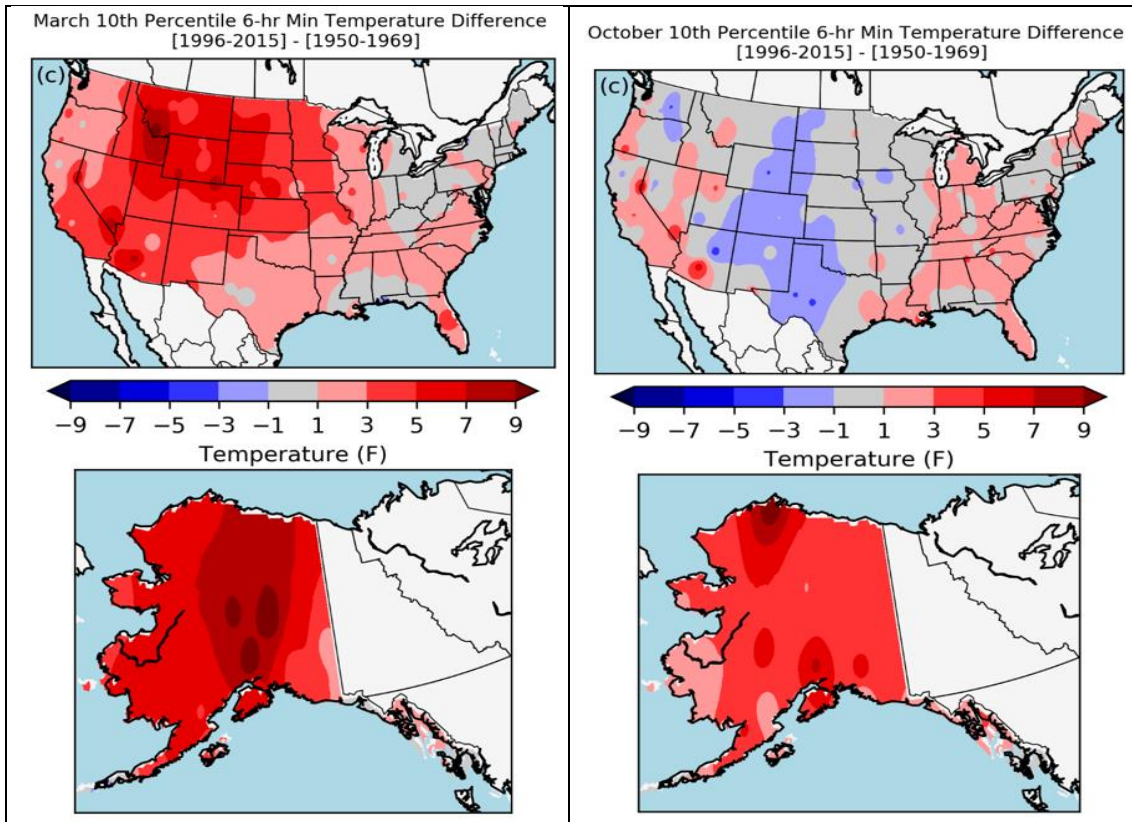
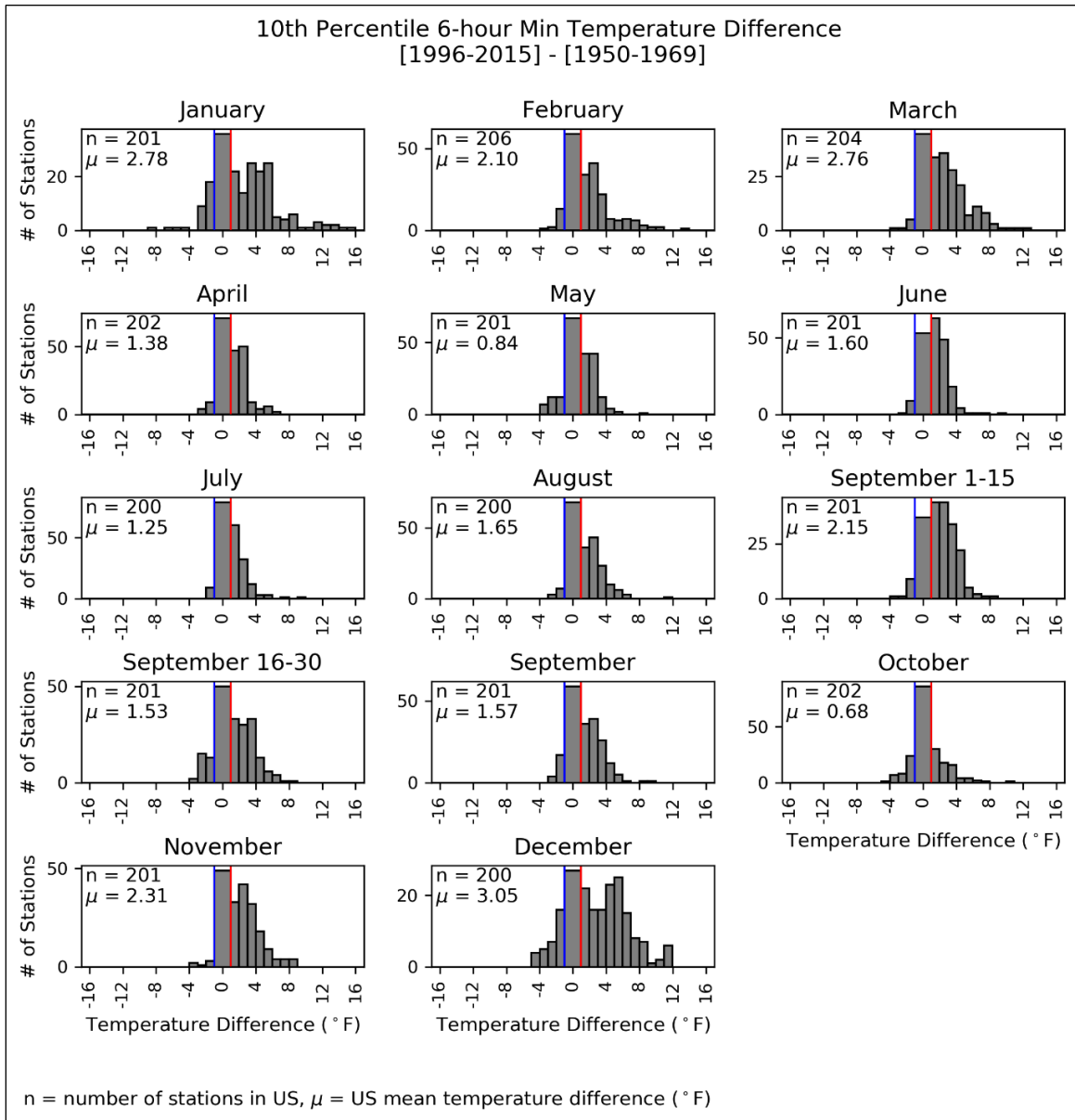


Figure 13. Interpolated maps showing differences in 10<sup>th</sup> percentile 6-hr min. temperature between Doner and Modern eras during March (left) and October (right).

### 4.3.2 Histograms

Histograms showing the numbers of stations exhibiting warming and cooling trends with respect to the 10<sup>th</sup> percentile 6-hr min. temperatures are provided, by month, in Appendix V-C. Histograms showing all the stations in the U.S. (excluding Hawaii) are presented in Figure 14. These histograms are similar to the 1-hr min. temperature histograms shown in Figure 10. In both cases, the months showing the largest overall warming are January, March, and December, while those showing the smallest overall warming are May and October.



**Figure 14. Numbers of weather stations throughout the U.S. showing differences in 10<sup>th</sup> percentile 6-hr min. temperature between the Doner and Modern eras (by month).**

In the warming months of January and March, over 85% of stations in the West Coast, Rocky Mountain, and Midwest regions show a warming trend. In December, however, stations in Alaska,

New England, Central Atlantic, and the Lower Atlantic regions drive the overall warming trend the most.

### 4.3.3 Statistical analysis of temperature differences

Differences between the 10<sup>th</sup> percentile 6-hr min. temperatures in the Doner and the Modern eras were analyzed statistically by month and geographic region. These differences, and their probability values (p-values), are given in Table 8. As the shading indicates, the majority of cells in this table (89 of 126) exhibit a warming trend of  $\geq 1.00$  °F between the two time periods. Only one cell indicates a cooling trend of  $\geq 1.00$  °F. All 90 of the highlighted differences shown in Table 8 are statistically significant to the 95% confidence level (p-value < 0.05), with 88 of the 90 being statistically significant to the 99% confidence level (p-value < 0.01).

**Table 8. Differences and associated p-values in 10<sup>th</sup> percentile 6-hr min. temperature between Doner and Modern eras (Modern – Doner)**

	US		AK		New England PADD 1A		Central Atlantic PADD 1B		Lower Atlantic PADD 1C		Midwest PADD 2		Gulf Coast PADD 3		Rocky Mountain PADD 4		West Coast PADD 5	
	°F	p	°F	p	°F	p	°F	p	°F	p	°F	p	°F	p	°F	p	°F	p
Jan	2.77	0.00	1.86	0.05	-0.41	0.29	-1.20	0.02	0.07	0.84	2.97	0.00	2.36	0.00	7.18	0.00	5.53	0.00
Feb	2.10	0.00	6.01	0.00	3.93	0.00	1.90	0.00	1.34	0.00	0.73	0.00	1.05	0.00	2.52	0.00	2.06	0.00
Mar	2.76	0.00	4.90	0.00	0.48	0.18	0.48	0.13	1.40	0.00	2.79	0.00	1.65	0.00	5.56	0.00	2.91	0.00
Apr	1.37	0.00	2.33	0.00	0.84	0.01	1.24	0.00	1.93	0.00	1.59	0.00	0.77	0.01	0.90	0.00	0.90	0.01
May	0.84	0.00	1.14	0.00	2.54	0.00	1.42	0.00	0.98	0.00	0.57	0.03	-0.02	0.94	-0.98	0.02	1.87	0.00
Jun	1.59	0.00	1.64	0.00	1.50	0.01	1.30	0.00	2.29	0.00	1.67	0.00	1.54	0.00	0.23	0.46	2.06	0.00
Jul	1.25	0.00	1.48	0.00	2.11	0.00	0.96	0.00	1.47	0.00	0.75	0.00	0.42	0.02	1.56	0.00	2.08	0.00
Aug	1.64	0.00	0.65	0.07	3.36	0.00	2.08	0.00	2.19	0.00	1.59	0.00	0.71	0.00	0.52	0.29	2.69	0.00
Sep 1-15	2.14	0.00	1.83	0.00	3.41	0.00	2.69	0.00	2.82	0.00	2.30	0.00	1.90	0.00	1.69	0.00	1.49	0.00
Sep 16-30	1.52	0.00	0.67	0.08	4.28	0.00	2.92	0.00	2.28	0.00	1.39	0.00	-0.73	0.02	1.67	0.01	1.75	0.00
Sep	1.57	0.00	0.78	0.03	3.59	0.00	2.36	0.00	2.14	0.00	1.63	0.00	0.10	0.73	1.57	0.00	1.65	0.00
Oct	0.68	0.00	3.52	0.00	1.23	0.01	0.12	0.75	1.37	0.00	0.13	0.46	-0.09	0.84	-0.37	0.39	0.60	0.15
Nov	2.30	0.00	3.68	0.00	0.55	0.10	0.78	0.03	2.06	0.00	3.42	0.00	2.10	0.00	1.64	0.00	1.56	0.00
Dec	3.05	0.00	7.71	0.00	6.14	0.00	5.51	0.00	4.40	0.00	3.62	0.00	0.71	0.04	-0.70	0.17	-0.39	0.34

Notes: Red-shaded cells indicate temperature warming of  $\geq 1.00$  °F (89 cells)  
 Blue-shaded cells indicate temperature cooling of  $\geq 1.00$  °F (1 cell)  
 Due to rounding, p-values shown as "0.00" indicate the values are <0.01

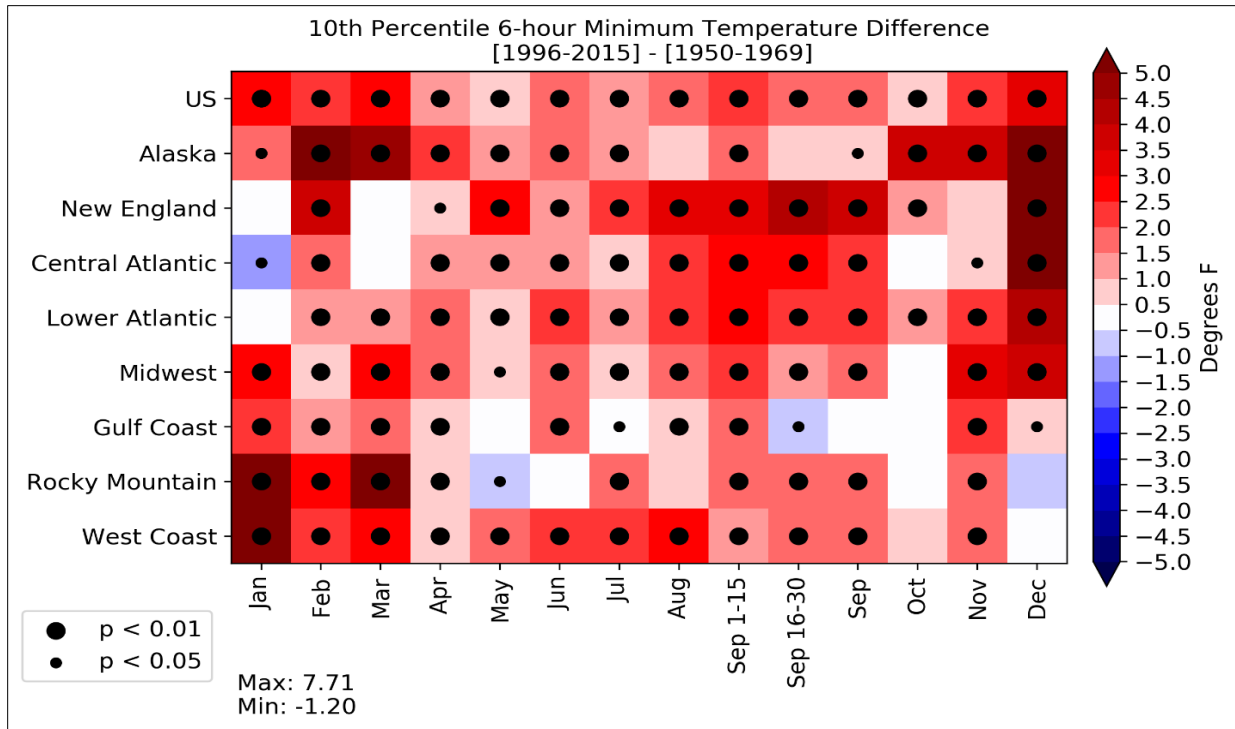


**Figure 15. Magnitude and significance of 10<sup>th</sup> percentile 6-hr min. temperature differences between the Doner era (1950-1969) and the Modern eras (1996-2015) – by month and PADD.** (Note: “p” refers to the statistical p-value. For grid cells showing no dot, p > 0.05.)

The checkerboard plot of Figure 15 provides a visual depiction of these statistical analyses. The single largest increase in 10<sup>th</sup> percentile 1-hr min. temperature of 7.71 °F occurs in Alaska in December. The largest temperature decrease of -1.20 °F occurs in PADD 1B (Central Atlantic) in January. As was true with the 10<sup>th</sup> percentile 1-hr min. temperatures, these 6-hr min. temperature values also show an overall warming trend throughout the entire U.S. in every month.

## 5 Conclusions

In this study, the original Doner methodology for determining ambient temperature patterns throughout the U.S. was successfully replicated for two different time periods: the Doner era (1950-1969) and the Modern era (1996-2015). For both time periods, monthly temperature patterns were defined using three temperature metrics: (1) 90<sup>th</sup> percentile 1-hr max., (2) 10<sup>th</sup> percentile 1-hr min., and (3) 10<sup>th</sup> percentile 6-hr min. Differences between the Doner and Modern temperature patterns exhibited large variability, both spatially and temporally.

While the overall results are consistent with a general warming trend occurring between the Doner and the Modern eras, the magnitude, spatial extent, and month of occurrence of warming are all variable. As shown in the checkerboard plots created to summarize the results, greater warming was seen in most locations and months when using metrics based on minimum temperatures as compared to maximum temperatures. This larger increase in minimum vs. maximum temperatures is consistent with the broader temperature change literature for the U.S. Cooling is seen in 3-5% of the checkerboard grid cells from the minimum temperature results, but in 14% of the grid cells from the maximum temperature results. Approximately 80% of the 31 cooling changes greater than 0.5 °F

seen in all three checkerboard plots were statistically significant to the 95% percent confidence level, whereas 90% of the 298 total warming changes greater than 0.5 °F were significant to the same confidence level.

The largest temperature increase seen with the 90<sup>th</sup> percentile 1-hr max. temperature data is 5.9 °F, occurring in PADD 2 (Midwest) during March. Of the 126 PADD-month combinations investigated, 69 show temperature warming greater than 0.5 °F, with 16 of these having warming in excess of 2.0 °F. The largest temperature decrease seen from the maximum temperature metric is -2.4 °F, occurring in PADD 2 in October. Of the 126 PADD-month combinations investigated, 20 show temperature cooling greater than 0.5 °F, with only one of these having cooling in excess of 2.0 °F.

The largest temperature increase seen with the 10<sup>th</sup> percentile 1-hr min. temperature data is 7.7 °F, occurring in Alaska during December. Ninety-six of the 126 PADD-month combinations investigated show warming in excess of 0.5 °F, with 35 of these having warming in excess of 2.0 °F. The largest temperature decrease seen for this minimum temperature metric is -1.5 °F, occurring in PADD 1B (Central Atlantic) during January. Only 7 of the 126 PADD-month combinations show cooling in excess of 0.5 °F, based on this minimum temperature metric.

While it is tempting to compare these temperature change results with other results reported in the broader climate change literature, this should be done with extreme caution. This study was undertaken to replicate the earlier Doner methodology as it relates to particular ASTM fuel specifications. For this reason, the study focused on extreme temperature metrics (90<sup>th</sup> percentile 1-hr max. and 10<sup>th</sup> percentile 1-hr min. temperatures) rather than daily average temperature values, which are generally the focus of climate change investigations. Furthermore, this study utilized temperature data from a relatively small number of weather stations at discrete locations (mostly airports and military facilities) that may not adequately represent the entire U.S. landmass. Broader climatological databases, such as that accessible through the NCEI *Climate at a Glance* tool (<http://www.ncdc.noaa.gov/cag>) include temperature data from many more stations.

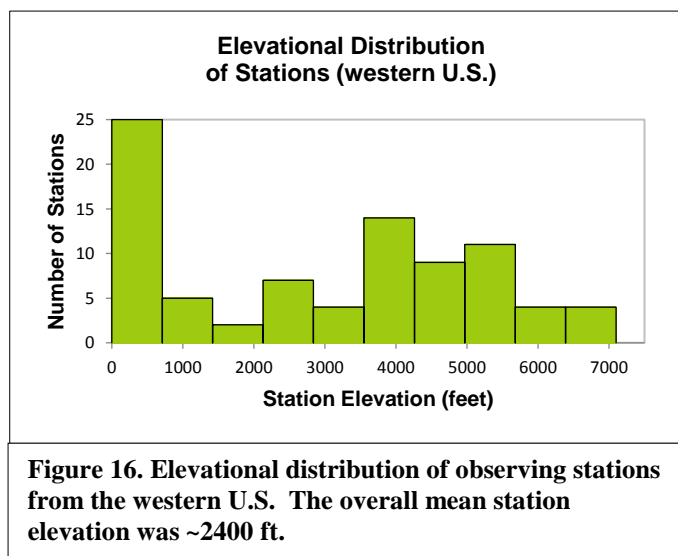
Application of the *Climate at a Glance* tool for the entire CONUS region during the Doner and Modern eras shows increases of 1.15°F and 1.57°F for annual maximum and minimum temperatures, respectively. Results from this study show increases of 0.65°F and 1.61°F for annual 90<sup>th</sup> percentile 1-hr maximum and 10<sup>th</sup> percentile 1-hr minimum temperatures, respectively. Perfect agreement is not expected, due to differences in temperature metrics and the number of stations used. Nevertheless, reasonably close agreement is expected (and observed), as the same NCEI-archived database is utilized in both cases.

It is unclear whether the temperature changes observed between the Doner and Modern eras are large enough to warrant a re-examination of fuel specifications that are based on ambient temperature conditions. However, if such a re-examination is to be undertaken, a more comprehensive analytical approach should be considered to define the spatial and temporal distributions of current ambient temperatures throughout the U.S. Elements of such a comprehensive approach are provided below in the Recommendations section of this report.

## 6 Recommendations

In this project, DRI successfully met the original objectives by completing a comparative analysis of air temperature data between the two specified time-periods of interest (1950-1969 and 1996-2015) while replicating the original Doner methodology. Certain limitations to the data analysis, however, were known at the outset, due to the requirement of adhering to the Doner methodology, specifically with respect to the number of weather stations available for analysis. After preliminary metadata inspection of the original stations was carried out and data completeness thresholds were applied, the total number of stations used in our analysis was reduced to about 220, as compared to the 340 stations Doner used. When analyzing the data on a geographic basis according to PADD regions, some regions were represented by a limited number of stations; e.g., PADD 1A (New England) has only 9 stations and PADD 4 (Rocky Mountain) has only 30 stations.

Another limitation due to the low spatial density of stations is the possible impact this has on the accuracy and precision of spatially interpolated maps. This is primarily a concern in the western U.S., an area of complex terrain where temperature cycles and extremes vary both spatially and temporally. Interpolated maps produced for this report show that mountain ranges are not adequately resolved spatially, which is due to the low station density and lack of high elevation stations being available. Not only does the total number of stations used impact the interpolation process results, but also the characteristics of the individual observing sites (e.g., station elevation, mountain vs. valley, coastal proximity, etc.) must be taken into consideration. The chosen site locations need to be spatially representative of the broader scale temperature patterns of a given geographic region. Many stations from the western U.S. used in this study are situated in relatively low elevation or valley locations, in close proximity to mountain ranges. The elevational distribution of the western stations is shown in Figure 16. These valley locations characteristically display different heating and cooling cycles and are often subject to extreme temperatures in relation to their geographic position and other topography-related processes; such as cold-air drainage pooling and temperature inversions.



The sophistication of climatological databases and analytical tools has increased since the time of the Doner report. To address the limitations identified in the present study, and to develop a more accurate and granular understanding of ambient temperature patterns, DRI recommends that some of these advanced tools and data sources be utilized. For example, the Applied Climate Information System (ACIS; [http://www.rcc-acis.org/docs\\_datasets.html](http://www.rcc-acis.org/docs_datasets.html)) provides access to over 10,000 daily weather stations in the U.S. that report daily minimum and maximum temperatures. From this system, it would be possible to determine desired percentile values for min. and max. temperatures at

much greater spatial resolution than in the Doner methodology. However, because ACIS provides only daily min. and max. temperatures, additional hourly information sources would be required to compute percentile values of 6-hr min. temperatures.

DRI also recommends using the 30-year climate normal period the World Meteorological Organization (WMO) has adopted to generate temperature distributions and percentiles.<sup>9</sup> The current 30-year period is 1981-2010 and new normals are computed once every ten years (i.e., the next normal period will be 1991-2020). Climate normals act to serve as a benchmark for the most recent climatic conditions.

A final recommendation is to use high-resolution gridded climate data, driven by ACIS observations, instead of using only individual stations. The Parameter Regression on Independent Slopes Model (PRISM)<sup>10</sup> could be used which, by design, integrates a larger number of stations from various networks (including additional stations outside of ACIS). PRISM applies a sophisticated multivariate interpolation scheme that takes into account other important climate-related elements such as elevation, coastal proximity, and slope orientation. The PRISM dataset has been extensively used within the scientific research community and by a wide variety of state and federal agencies including the National Weather Service and the U.S. Department of Agricultural, where it serves as their official climatological dataset. Overall, this would provide more robust basis to examine the modern period that could serve to more effectively guide the process of evaluating existing gasoline volatility classifications.

As an illustration, the 1981-2010 normal annual maximum temperatures PRISM map is shown in Figure 17. Note that the data shown in Figure 17 have no relevance to either the original Doner study or the current DRI study.) Over 15,000 weather stations were used to generate this map. Terrain features, particularly in the western US, are clearly visible due to the high resolution of the data (4 km spatial resolution). A 30-year normal map is shown, but PRISM is generated at daily temporal resolution. A current limitation of PRISM is its lack of availability for Alaska and Hawaii, although the ACIS station database could still be used for those states.

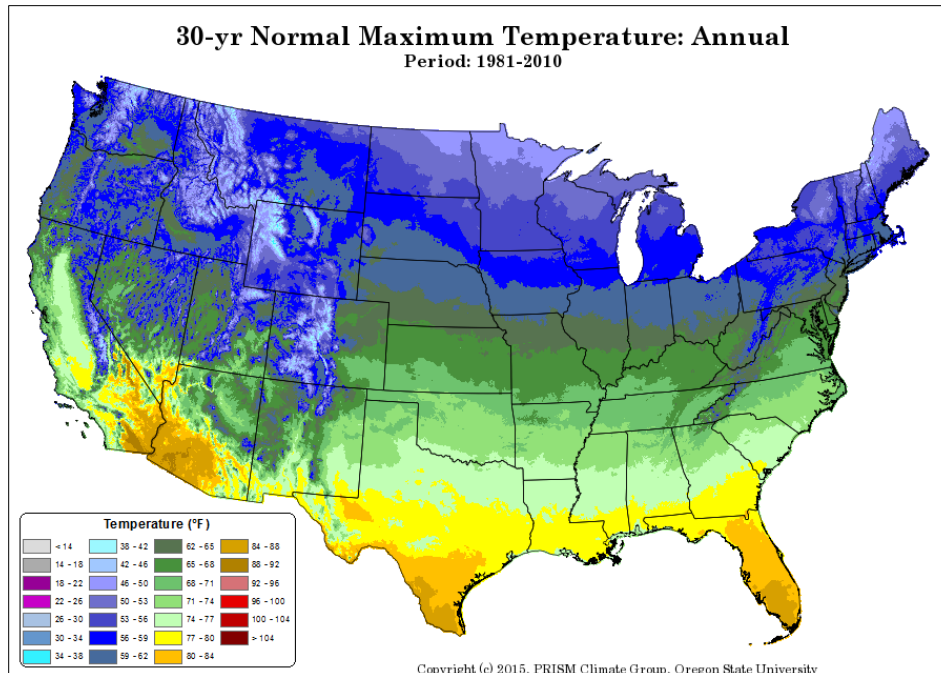


**Figure 17. PRISM 30-year normal annual maximum temperature downloaded from <http://prism.oregonstate.edu/normals/>.**

## 7 References

1. ASTM D4814-18a, "Standard Specifications for Automotive Spark Ignition Engine Fuel," ASTM International, West Conshohocken, PA, April, 2018.
2. "A Predictive Study for Defining Limiting Temperatures and their Application in Petroleum Product Specifications," John P. Doner, U.S. Army Mobility Equipment Research and Development Center, Aberdeen Proving Ground, Maryland, CCL Report No. 316, November 1972.
3. ASTM D975-18, "Standard Specifications for Diesel Fuel Oils," ASTM International, West Conshohocken, PA, April, 2018.
4. Oke, T.R. (1973). City size and the urban heat island. *Atmospheric Environ.* **7** (8), 769-779. DOI: 10.1016/0004-6981(73)90140-6.
5. Hatchett, B.J., Koracin, D., Mejia, J.F., and Boyle, D.P. (2016). Assimilating urban heat island effects into climate projections. *J. Arid Environments* **128**, 59-64. DOI: 10.1016/j.jaridenv.2016.01.007.
6. Diaz, H.F. and Bradley, R.S. (1997). Temperature variations during the last century at high elevation sites. *Climatic Change* **36**, 253-279. DOI: 10.1023/A:1005335731187.
7. Pepin, N., Bradley, R.S., Diaz, H.F., et al. (2015). Elevation-dependent warming in mountain regions of the world. *Nature Climate Change* **5** (5), 424-440. DOI: 10.1028/nclimate2563.
8. Samanta, S., Pal, D.K., Lohar, D., and Pal, B. (2012). Interpolation of climate variables and temperature modeling. *Theo. Appl. Climatol.* **107**, 35-45. DOI 10.1007/s00704-011-0455-3.
9. Arguez, A. and Vose, R. S. (2011). The definition of the standard WMO climate normal: The key to deriving alternative climate normals. *Bulletin of the American Meteorological Society*, **92** (6), 699-704. DOI: 10.1175/2010BAMS2955.1
10. Daly, C., Neilson, R. P. and Phillips, D. L. (1994). A statistical-topographic model for mapping climatological precipitation over mountainous terrain. *Journal of Applied Meteorology*, **33** (2), 140-158. DOI: 10.1175/1520-0450(1994)033<0140:ASTMFM>2.0.CO;2